AD-A167 005 INTERNAL PERFORMANCE OF A VARIABLE RAMP MIXED COMPRESSION INTAKE AT MACH 305(U) AERONAUTICAL RESEARCH LABS MELBOURNE (AUSTRALIA) S A FISHER AUG 85 1/1

UNCLASSIFIED ARL/AERO-PROP-R-167 F/G 21/5 NL

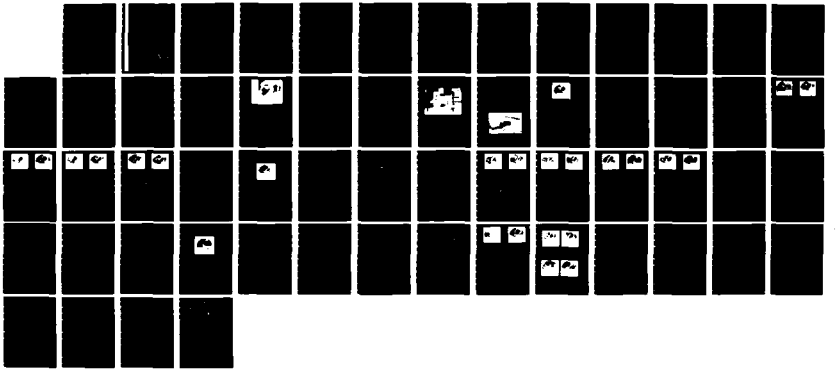

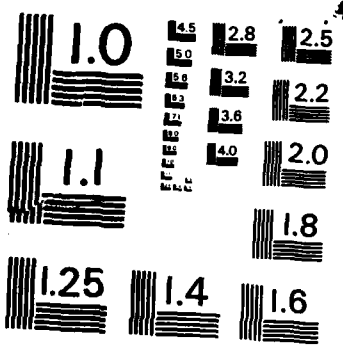

ARL-AERO-PROP-R-167 AR-004-041

DEPARTMENT OF DEFENCE

DEFENCE SCIENCE AND TECHNOLOGY ORGANISATION

AERONAUTICAL RESEARCH LABORATORIES

MELBOURNE, VICTORIA

Aero Propulsion Report 167

INTERNAL PERFORMANCE OF A VARIABLE RAMP MIXED COMPRESSION INTAKE AT MACH 3.05

by

S.A. FISHER

Approved for Public Release

COPY No

AUGUST 1985

AR-004-041

DEPARTMENT OF DEFENCE
DEFENCE SCIENCE AND TECHNOLOGY ORGANISATION
AERONAUTICAL RESEARCH LABORATORIES

Aero Propulsion Report 167

INTERNAL PERFORMANCE OF A VARIABLE RAMP MIXED COMPRESSION INTAKE AT MACH 3.05

by

S.A. FISHER

SUMMARY

Results are presented of an experimental investigation into the performance of a two-dimensional mixed compression intake which featured focussed cowl compression matched to a discrete slot boundary layer bleed system. The tests were conducted at the intake design Mach number of 3.05. The design worked well in a two-dimensional sense, but the losses were exacerbated by three-dimensional viscous effects involving the sidewall boundary layers.

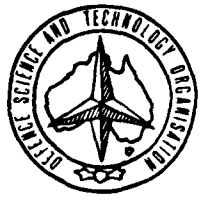

POSTAL ADDRESS: Director, Aeronautical Research Laboratories,
P.O. Box 4331, Melbourne, Victoria, 3001, Australia.

CONTENTS

		Page No.:
1.	INTRODUCTION	1
2.	MODEL GEOMETRY	1
3.	TEST APPARATUS	2
3.1	Wind tunnel	2
3.2	Controls and instrumentation	3
4.	RESULTS AND DISCUSSION	3
4.1	Variation of bleed slot design	3
4.2	Performance of configuration A	4
4.3	Performance of configuration B	6
4.4	Performance of configuration C	8
4.5	General discussion	9
5.	CONCLUSION	10

REFERENCES

FIGURES

DISTRIBUTION

DOCUMENT CONTROL DATA

NOTATION

H_i Intake model capture height - see Fig 1

P_s Static pressure

P_t Total pressure

P_{to} Tunnel stagnation pressure

Q_c Cowl bleed mass flow/Intake capture mass flow %

Q_r Ramp bleed mass flow/Intake capture mass flow %

t Ram scoop at ramp bleed slot - see Fig 1

δ_2 Deflection at supersonic ramp hinge, degrees - see Fig 1

η_{cr} Diffuser exit area mean P_t/P_{to} at critical.

1. INTRODUCTION

The range of possible design options in an engine air intake increases with maximum flight speed. For high Mach number operation, external drag considerations generally dictate that some of the supersonic compression should occur internally, at the cost (relative to fully external compression designs) of reduced operating flexibility and more demanding requirements for limiting internal flow separation and viscous losses. With two-dimensional configurations in particular, the sidewalls represent added internal surface area wetted by supersonic flow, providing for more boundary layer growth upstream of the throat and adding to the problem of boundary layer control in the region of maximum adverse pressure gradient.

An experimental investigation was undertaken to examine the extent of such problems in a two-dimensional mixed compression intake featuring a highly concentrated internal compression field which minimised both the length of the supersonic diffuser and the supersonic wetted area, and which could be matched to a simple slot bleed system. This involved an internal compression arrangement with focussed cowl shocks which, in broad terms, was a two-dimensional equivalent of the axisymmetric arrangement described in Reference 1. In comparison with some other designs which employ long internal contractions to limit the adverse pressure gradients throughout the supersonic diffuser (Refs 2 and 3, for example), this approach offers the attractions of overall compactness and potential simplicity of boundary layer control. In the case of the work reported in Reference 1 it also yielded economy of bleed mass flow rate.

The vehicle for the present study was a variable ramp intake model which was tested at its design Mach number of 3.05.

2. MODEL GEOMETRY

A photograph of the intake model, which had a capture area approximately 70 mm square, is shown in Figure 1(a). A sectioned elevation of the model appears in Figure 1(b), which also defines the more important geometric variables. The internal profiles of the supersonic diffuser are shown in more detail in Figure 2, together with the theoretical shock system for the "design" geometry, corrected for the displacement effect of the boundary layers on the ramp and cowl surfaces using figures derived from Reference 4. The relative strengths of the six oblique shock waves are indicated in the Figure by local surface angles and Mach numbers. Including the loss due to a normal shock occurring at the terminal supersonic Mach number of 1.43, the total pressure recovery through the complete shock system was 0.895.

The four internal oblique shock waves were designed to focus near the downstream edge of the ramp bleed slot, formed at the duct throat by the gap between the supersonic and subsonic diffuser ramps. The width of the slot at the design ramp angle was initially set at approximately half the throat height, but was subsequently varied as described later in Section 4.1. A second (flush) bleed slot positioned on the cowl side of the throat had a width equal to about 10 per cent of the throat height.

There was no provision for direct control of the boundary layers on the sidewalls. It was anticipated that a measure of indirect control would be achieved through the agency of local secondary flows of the type described in Reference 5, which involved migration of the sidewall boundary layers towards the ramp bleed slot under the influence of the pressure gradients associated with the internal supersonic compression field. A benefit of experimental convenience which accrued from this approach was the facility for uninterrupted schlieren observation of the flow in the intake throat, through the circular windows which are visible in Figure 1(a).

The sidewall leading edges lay in the plane intersecting the tips of the cowl and ramp. They were externally chamfered at 2.1 degrees in the plane parallel to the free stream flow direction, an angle sufficiently low to ensure attachment of the leading edge shock waves. The sidewalls remained internally flat and parallel for the full length of the model, there being no transition of the duct cross section to the circular shape which would be required if a turbine engine installation were to be fully simulated.

The length of the subsonic diffuser was 5.1 times the supersonic capture height, made up of three equal lengths with divergence angles at the design geometry (in one plane only) of 1.5, 4.5 and 9 degrees respectively. The exit Mach number was theoretically about 0.2, a relatively low figure for most applications.

The streamwise distribution of flow cross sectional area over the full length of the model is shown in Figure 3, for three different positions of the hinged ramps. Approximately 50 per cent of the supersonic area contraction occurred internally; ie. downstream of the cowl lip.

3. TEST APPARATUS

3.1 Wind Tunnel

The specialised wind tunnel used for the tests is described in detail in Reference 6. It employed the so-called spill diffuser principle, wherein the intake model formed an integral part of the tunnel diffuser. This permitted the use of a much larger model than could normally be accommodated in a conventional tunnel of equivalent size - the intake captured about one third of the total tunnel flow - at the expense of somewhat limited operating flexibility and inability to simulate the external flow about the model downstream of the capture plane. Access for schlieren observation was limited to the intake throat and cowl lip regions, the former being viewed through a series of six separate glass windows. The photograph in Figure 4 shows the model and diffuser assembly withdrawn from the tunnel working section, with one outer wall of the spill diffuser removed.

The tunnel stagnation pressure was 650 kPa which, at the test section Mach number of 3.05, gave a model Reynolds number based on intake capture height of 2.64×10^6. The tests were performed at only one value of Mach number, and at zero incidence.

3.2 Controls and Instrumentation

The variable intake ramps were positioned by reversible electric motors, and could be adjusted independently while the tunnel was in operation. Their positions were indicated remotely by linear variable differential transformers. The flows passing through the subsonic diffuser and the two bleed passages were separately metered by orifice plates and controlled by electrically operated valves.

Static pressure tappings were distributed on the centrelines of both upper and lower internal surfaces of the model. There was a 20-point pitot array positioned at the exit of the subsonic diffuser, with its probes distributed on an equal area basis, and for some tests there were three small pitot rakes mounted on the upper (cowl), lower (ramp) and sidewall surfaces immediately downstream of the model throat, as shown in Figure 5. Pitot probes were also installed in the two bleed passages. All pressures were recorded using pressure scanning valves, strain gauge transducers and automatic data acquisition equipment.

4. RESULTS AND DISCUSSION

4.1 Variation of Bleed Slot Design

Figure 6(a) shows a schlieren photograph of the flow in the throat of the model in its datum configuration, with the ramps set in their design positions, the bleed control valves fully open and the intake running supercritical; ie with the throat flow free from influence of any diffuser back-pressure. Whilst there is some evidence of interaction between shock waves and the sidewall boundary layers, the flow appears to be basically two-dimensional, as depicted in the interpretation shown in Figure 6(b).

An obvious departure from the design shock configuration is the position of the focus of the four cowl shocks, well upstream of the subsonic ramp tip. The degree of flow turning required to balance the pressure across the region of interaction of the cowl shocks with the shear layer spanning the ramp bleed slot, coupled with the geometry of the slot and the limited swallowing capacity of the ramp bleed system, dictated an extraneous oblique shock wave emanating from near the upstream edge of the bleed slot. As will be seen later, the position of this oblique shock was sensitive to both ramp geometry and back pressure, and sometimes created quite gross departures from the design shock configuration. In some circumstances there was pronounced three-dimensional interaction of the extraneous shock wave with the sidewall boundary layers, and when intake "unstart" occurred it always commenced with upstream movement of this shock.

With the purpose of realising more closely the design shock system, two additional variants of the ramp bleed slot geometry were included in the test programme. Both were based on the philosophy of isolating the bleed slot from the pressure rise associated with the cowl shocks. Figure 7 shows these two variants (B and C) compared with the datum configuration (A), along with the experimentally observed position of the cowl compression field. In both designs the cowl flow turning was accommodated

over a finite curved length of ramp surface (rather than at a point coinciding with the subsonic ramp tip, as was the intention with the datum configuration) and in both cases the region of curvature was preceded by a short lip with its upper surface approximately parallel to the supersonic ramp surface. Configuration C was designed to operate with a small degree of "ram scoop", namely $t/H_i = 0.02$ at $\delta_2 = 8^0$.

4.2 Performance of Configuration A

The pressure recovery performance of the datum configuration is summarised in Figures 8 and 9. The area mean critical pressure recovery at the diffuser exit is plotted against both supersonic ramp angle and ramp bleed slot geometry in Figure 8, and against bleed mass flow rates in Figure 9. With a fixed supersonic ramp angle δ_2, the ramp bleed flow could be varied either by moving the subsonic ramp (ie varying the dimension t) or by varying the opening of the appropriate control valve. Both effects are included in the upper graph of Figure 9. In the case of the cowl bleed, all of the variation shown in Figure 9 was achieved by means of the control valve.

Each of the experimental points plotted in Figures 8 and 9 was obtained by first setting the model geometry and then closing the main diffuser throttle valve until the intake was judged to be on the verge of "unstart". Some of the experimental scatter on the graphs is almost certainly due to small variations in the supercritical flow margins associated with this technique. There was also a degree of uncertainty in the positioning of the tip of the subsonic ramp, due to deflection of this component under the substantial pressure loads imposed on it. This effect was taken into account in the final analysis of the results, using numerous measurements from schlieren photographs, but the difficulty experienced in setting the ramp tip to a prescribed position is reflected in the width of the band of values of t/H_j for which the upper graph in Figure 8 applies, and in the correspondingly wide scatter of experimental points on that graph.

Some insight into the trends displayed in Figures 8 and 9 can be gained by reference to the wall static pressure distributions, schlieren photographs and diffuser exit flow distributions shown in Figures 10 to 13, which highlight the effects of supersosnic ramp angle, ramp bleed slot geometry, ramp bleed throttle opening and cowl bleed flow respectively. Each of this group of Figures contains data relating to a pair of experimental points identified by circled numbers on the appropriate graph in Figures 8 and 9. Aspects worthy of particular note are:

(a) Comparative levels of mean total pressure recovery always correlated with the static pressure rise in the intake duct, which could be broadly divided into the pressure rise in the supersonic diffuser, the pressure rise through the transition to subsonic flow in the throat and the pressure rise in the subsonic diffuser. As well as measured wall pressures, Figures 10 to 13 include for comparison the theoretical inviscid static pressure distribution for $\delta_2 = 8^0$, calculated assuming that a clean normal shock was ideally located in the intake throat.

(b) The wall static pressures in the supersonic diffuser generally showed the expected level of agreement with theoretical values, although the two pressures registered at the tappings closest to the throat on both the cowl and ramp sides were sometimes influenced by the extraneous oblique shock wave ahead of the ramp bleed slot when its origin was forced upstream.

(c) The static pressure rise in the throat always fell well short of the theoretical value. This can be partly explained by departures from the theoretical shock pattern, but is thought also to have been associated with three-dimensional viscous flow effects which are not evident in the data of Figures 10-13. Further discussion of this aspect follows later.

(d) The static pressure rise in the subsonic diffuser was less sensitive to geometry and throat bleed than was the pressure rise in the throat. As would be expected, however, there was a tendency towards reduced subsonic diffuser effectiveness with highly distorted flow distributions. In Figure 12, for example, throttling the ramp bleed flow is seen to have reduced the overall pressure rise despite increased pressure at the throat; this was accompanied by increased distortion of the diffuser exit flow, as illustrated qualitatively by the isobaric plots of local mean total pressure recovery at the bottom of the Figure. No doubt the flow distortion at the entry of the subsonic diffuser was correspondingly increased.

(e) The diffuser exit flow distributions almost invariably exhibited distortion of the more energetic flow towards the cowl side of the duct. Two effects which commonly exacerbated this tendency were partial obliteration of the cowl compression field on the ramp side of the throat due to upstream movement of the extraneous oblique shock (eg Figure 10) and failure of the ramp bleed slot to capture sufficient proportion of the ramp boundary layer flow (eg Figure 11).

(f) The ramp bleed flow could be throttled to only a limited degree before the extraneous oblique shock was forced upstream to the point of expulsion, leading to intake "unstart". Although partly obscured by dirty windows, this effect is evident in the schlieren photographs in Figure 12.

(g) The progressive increase in critical point pressure recovery which accompanied throttling of the cowl bleed flow was unexpected. This trend appears to have been due in part to weakening of the expansion/shock wave combination associated with flow deviations which existed near the cowl bleed slot when the bleed was open (see Figure 6). The local shock losses were thus reduced, with no apparent corresponding increase in viscous losses. Additional benefit accrued from an ability to position the terminal shock further upstream in arriving at the "critical" condition, as the bleed was

throttled. The absence of any benefit from cowl bleed was consistent with the findings of References 1 and 7 in which the test geometries, like that of the present investigation, were designed with minimum length cowls using focussed cowl compression. Both reported optimum overall performance with zero cowl bleed.

The presentation of experimental data for the datum configuration is completed by the graphs of cowl and ramp bleed pressure recovery plotted against ramp angle and ramp bleed slot geometry in Figure 14. Both recoveries were determined from the pressures registered by the single pitot probe located in each bleed passage. As would be expected, the ramp bleed recovery exhibited much greater sensitivity to the geometric variables than did the cowl bleed recovery.

4.3 Performance of Configuration B

Figure 15 shows a schlieren image of supercritical throat flow recorded with ramp bleed slot configuration B. This is directly comparable in terms of other geometric variables with the photograph which relates to configuration A, in Figure 6(a). The ramp bleed passage is now effectively isolated from the influence of the cowl supersonic compression, so that the extraneous oblique shock upstream of the bleed slot has been eliminated. However, the cowl compression field is by no means cancelled where it impinges on the curved lip of the subsonic ramp, and its interaction with the reflected shock generates a visible shear layer flowing downstream into the subsonic diffuser.

The critical pressure recovery performance is shown plotted against variable geometry and bleed flow in Figures 16 and 17 respectively. Testing of configuration B covered a much larger range of ramp angle than did that of configuration A, mainly because bleed slot B (unlike A) remained reasonably well matched to the shock system to higher values of δ_2.

With a fixed value of δ_2, ramp bleed flow in Configuration B could again be varied either by changing the degree of "ram scoop" at the bleed slot or by throttling the bleed flow, both effects being included (for one value of δ_2) in Figure 17. In view of the relatively poor rate of exchange between pressure recovery and bleed flow over the upper portion of the curve connecting the solid symbols, it is unlikely that the "fully open" position of the ramp bleed valve would provide the best level of thrust minus drag in a full propulsion system analysis. Previous studies (Refs 8, 9) suggest that for overall benefit at Mach 2.5 - 3 cruise conditions, a 1 per cent increase in bleed flow in a mixed compression intake should yield at least 1 per cent improvement in pressure recovery. It is likely, therefore, that an "optimum" set of performance curves equivalent to that in Figure 17 would be obtained with partially throttled ramp bleed (and zero cowl bleed, as with configuration A) and, in terms of ramp bleed mass flow, would lie about 1 ½ percentage points to the left of the family of curves in Figure 17.

Notwithstanding the above, pressure recovery performance with both bleed valves fully open is summarised by the cross plots in Figure 18, which also includes a curve of theoretical shock recovery versus ramp

angle calculated from surface geometry alone; ie totally ignoring boundary layer effects. The "extra-to-shock" loss appears to correlate closely with ramp bleed flow, the minimum recorded being about 10 per cent of the free stream total pressure with 8 per cent ramp bleed. This figure, sometimes referred to as the "viscous loss", is somewhat higher than might be expected in a high performance intake.

The effects of geometry and bleed flow on the throat flow pattern and on the diffuser static pressure and exit total pressure distributions are shown in Figures 19-22. As was the case with the presentation of corresponding data for configuration A, each of these Figures relates to a selected pair of experimental points identified by circled numbers on appropriate graphs in Figures 16 and 17. The data in Figures 19-22 is in this case augmented by profiles of total pressure measured at the throat pitot rakes, shown plotted in Figures 23-26 respectively.

In discussing Figures 19-26, many of the observations made in Section 4.2 could be repeated. Other points worth noting are:

(a) An oblique shock appeared at the upstream edge of the ramp bleed slot only when the ramp bleed flow was throttled (Figure 21). Instead, there was invariably a shock wave which appeared to be of substantial strength attached at or near the leading edge of the subsonic ramp.

(b) There was evidence of departure from two-dimensional flow in the throat region, in the form of multiple shock wave images suggesting non-planar shocks (eg the two schlieren photographs in Figure 19).

(c) Although displaced from one another both laterally and streamwise (see Figure 5), the throat rakes C and R registered pressures which generally were sufficiently well matched to justify a continuous curve through all ten points to represent the vertical profile of total pressure across the duct. Values of local total pressure in the bulk of the flow always exceeded the theoretical inviscid value by a small margin, probably because of a tendency for viscous effects at the wall to increase shock recovery outside the viscous region.

(d) Variation of geometry and bleed flow generally had the expected qualitative effect on the vertical throat profiles, at least on the ramp side of the duct. Cowl side effects were both less pronounced and less predictable.

(e) The levels of throat pressure recovery in Figure 23 show that the benefit of increasing δ_2 was due less to a general increase in shock recovery (as a simple theoretical prediction might suggest) than to improved matching of the shock system to the ramp bleed location and increased ramp bleed flow.

(f) Not only did local values of throat pressure recovery compare well with the theoretical shock recovery, but with favourable settings of geometry the vertical flow profiles at the throat appeared to be quite healthy and well equipped to negotiate the pressure rise in the subsonic diffuser. The high level of extra-to-shock loss is thought to be associated with three-dimensional flows originating at the throat, which are described in a more detailed analysis of the flow outlined in References 10 and 11.

(g) These three-dimensional effects can be seen in the total pressure profiles measured at rake S, which were generally characterised by relatively high energy flow adjacent to the surface and a trough in measured total pressure at about rake mid-span. These features are thought to have been associated with a streamwise vortex originating near each end of the ramp bleed slot. It is argued in References 10 and 11 that the two vortices had a significant influence on the subsonic diffuser flow, including the exit plane distortion, and that one of the pair had a major effect on the profile measured at rake S. The magnitude of some of the pressures registered at the rake are likely to have been influenced by local flow direction as well as velocity and static pressure, and substantial variations occurred in the profile shape as changes in geometry and/or bleed flow affected the position and/or strength of the vortices. This had the somewhat incongruous effect that a given variation in geometry or ramp bleed produced a change in the general level of measured pressure at rake S which was usually opposite in sign to the corresponding change in η_{cr}.

The bleed pressure recoveries for configuration B are shown as functions of geometry in Figure 27. The cowl bleed recovery was much the same as for configuration A, but the ramp bleed recovery was somewhat reduced, due to the absence of the oblique shock at the upstream edge of the ramp bleed slot.

4.4 Performance of Configuration C

The schlieren photograph in Figure 28 shows how ramp bleed slot configuration C was matched to the shock system at supercritical conditions. Figures 29 and 30 show how critical pressure recovery varied with bleed flow and geometry. In this case the performance is shown only for the "fully open" position of both bleed valves, the limited tests which were performed with throttled bleed having indicated behaviour which was similar to that of configuration B in this respect. Pressure recovery performance is summarised and compared with theoretical inviscid shock recovery in Figure 31, and bleed pressure recovery is shown in Figure 32.

Detailed results of pressure measurement and flow visualisation for configuration C are not presented. These displayed generally similar features to the results observed with configuration B. One noticeable difference in the behaviour of configuration C, however, is seen in the pronounced flattening of the pressure recovery v^s ramp bleed flow curves for values of Q_r above about 5 ½ per cent (Figure 30), compared with the continuing rising trend displayed by the curves in Figure 17. It seems evident that the potential benefit of increased ramp bleed flow rates above this level was not realised with the relatively high degree of "ram scoop" necessary to achieve such flow rates. Figure 33 compares throat flow patterns and total pressure profiles for configurations B and C, with identical supersonic ramp angles and comparable (relatively high) levels of ramp bleed flow. The two corresponding experimental points in Figures 17 and 30 are identified by the circled numbers 17 and 18 respectively. The profiles measured at rake R reveal generally inferior local total pressure recovery in configuration C, apparently due (at least in part) to the relatively strong shock wave at the subsonic ramp tip and interference of this shock wave with the cowl compression field. Also, with the higher values of t/H_j, when the ramp tip shock was strongest, unstart was generally initiated by upstream motion of that shock while the terminal shock wave was still some distance downstream of the throat. This would have further depressed the "critical point" recovery in Configuration C at these conditions.

Figure 34 shows four schlieren photographs of the throat flow, all taken at nominally the same condition but with the optical cut-off in four different positions disposed 90^0 apart. Amongst features of the flow which are revealed with varying emphasis as the cut-off is changed, are three-dimensional effects due to the surface boundary layers. These include the apparent "thickening" of the four cowl shocks (especially the lip shock) and the presence of oblique shocks (and their reflections) apparently originating from the supersonic ramp surface upstream of the circular windows. These phenomena are discussed in more detail in References 10 and 11, which include the results of surface flow visualisation showing three-dimensional separation of the sidewall boundary layers at the lip shock, and viscous effects in the ramp/sidewall corner well upstream of the bleed slot.

4.5 General Discussion

The pressure recovery/bleed flow performance of the three configurations tested is compared in Figure 35, for four different values of the supersonic ramp angle δ_2. Bleed slot A yielded peak values of pressure recovery which compared well with the other two configurations at the lower ramp settings. However, relatively high bleed flow rates were needed to achieve these values, a fact which is consistent with the observed poor matching of the bleed slot geometry with the shock system. The quality of this matching deteriorated further with increasing ramp angle, to the extent that the peak pressure recovery also deteriorated. The performance of the other two configurations improved with increasing ramp angle.

Bleed slots B and C yielded very similar levels of performance with low rates of bleed flow. As discussed in the previous Section, however, as ramp bleed was increased (by increasing t/H_i) a point was reached where configuration B failed to respond with significant further improvement in pressure recovery. At this stage the performance curves for the two geometries diverged, as seen in Figure 35.

The minimum "extra-to-shock" loss based on area mean pressure recovery was about 10 per cent of the free stream total pressure, as previously observed in relation to Figure 18, with bleed slot B. This figure decreased to about 9 per cent when calculated in terms of mass weighted mean recovery, and would have been further reduced had all of the results been measured with zero cowl bleed. The ramp bleed flow rate required to achieve this level of performance, about 8 per cent of the total capture mass flow, was consistent with a correlation of bleed flow rate required for optimum performance based on the ratio of internal supersonic wetted area to throat cross sectional area which is developed in Reference 8, for both axisymmetric and two-dimensional mixed compression intakes designed for Mach numbers between 2.5 and 3.5.

5. CONCLUSION

Results relating to critical point performance have been presented for a range of intake geometries, including three different arrangements for matching the ramp bleed slot to the supersonic compression field. With the better matched arrangements, the focussed cowl compression system appeared to work well in a two-dimensional sense; ie judged in terms of centreline wall static pressures in the supersonic diffuser, schlieren observation and throat flow profiles measured remote from the sidewalls. However, the extra-to-shock loss measured at the diffuser exit plane - about 10 per cent of the free stream total pressure with 8 per cent ramp bleed, based on area mean recovery - was greater than might be expected in a high performance intake.

The extra-to-shock loss correlated closely with the deficiency in static pressure rise in the model throat, and was to some degree attributable to three-dimensional viscous effects in that region which affected the exit flow distribution as well as the total pressure recovery. The anticipated difficulty of controlling sidewall boundary layer effects in this type of design was thus confirmed. Detailed investigation of this aspect, and further development of the design, are described in a separate report.

REFERENCES

1. J.F. Wasserbauer, R.J. Shaw, H.E. Neumann — Minimising boundary layer bleed for a mixed compression inlet. AIAA/SAE, Propulsion Joint Specialist Conference, Las Vegas, Nov 1973.

2. N.E. Sorensen, D.B. Smeltzer, E.A. Latham — Advanced supersonic inlet technology J. Aircraft Vol 10 No 5, May 1973.

3. J. Syberg, J.L. Koncsek — Experimental evaluation of a Mach 3.5 axisymmetric inlet. NASA CR-2563, July 1975.

4. W.H. Schofield — Theoretical investigation of boundary layer development in a two-dimensional mixed compression intake. Aeronautical Research Laboratories Note ARL/ME 280, August 1966.

5. M.C. Neale, P.S. Lamb — Tests with a variable ramp intake having combined external/internal compression and a design Mach number of 2.2. Aeronautical Research Council C.P. No 805, 1965.

6. S.A. Fisher, D.J. Ford — An investigation of starting problems in a specialised wind tunnel for testing a rectangular mixed compression intake at Mach 3. Aeronautical Research Laboratories Report ARL/ME 138, June 1972.

7. R.J. Shaw, J.F. Wasserbauer, H.E. Neumann — Boundary layer bleed system study for a full-scale, mixed-compression inlet with 45 per cent internal contraction. NASA TM-X-3358, March 1976.

REFERENCES (CONT'D)

8. D.N. Bowditch — Some design considerations for supersonic cruise mixed compression inlets. AIAA/SAE, Propulsion Joint Specialist Conference, Las Vegas, Nov 1973.

9. E. Tjonneland — The design, development and testing of a supersonic transport intake system. AGARD CP-91-71, Sept 1971.

10. S.A. Fisher — Three-dimensional flow effects in a two-dimensional air intake with mixed supersonic compression. Proc. 7th International Symposium on Air Breathing Engines, Beijing, Sept 1985.

11. S.A. Fisher — Investigation of three-dimensional flows in a variable ramp mixed compression intake at Mach 3:05. Aeronautical Research Laboratories Report in course of preparation.

(a) Photograph of model

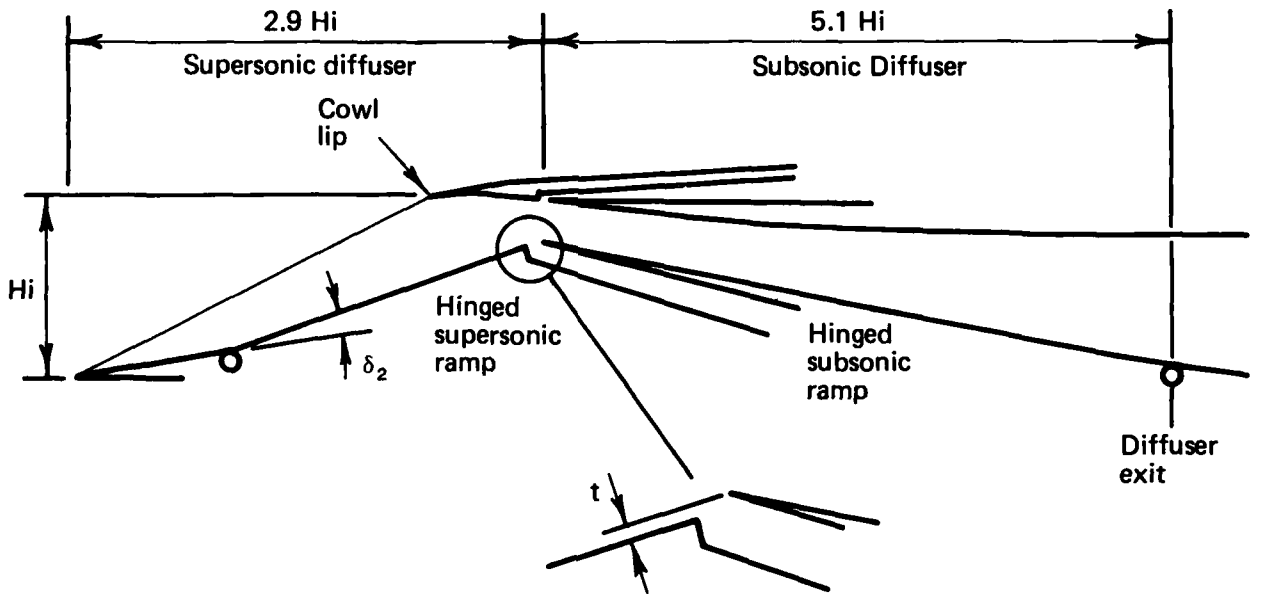

(b) Internal profiles

FIG. 1 INTAKE GEOMETRY

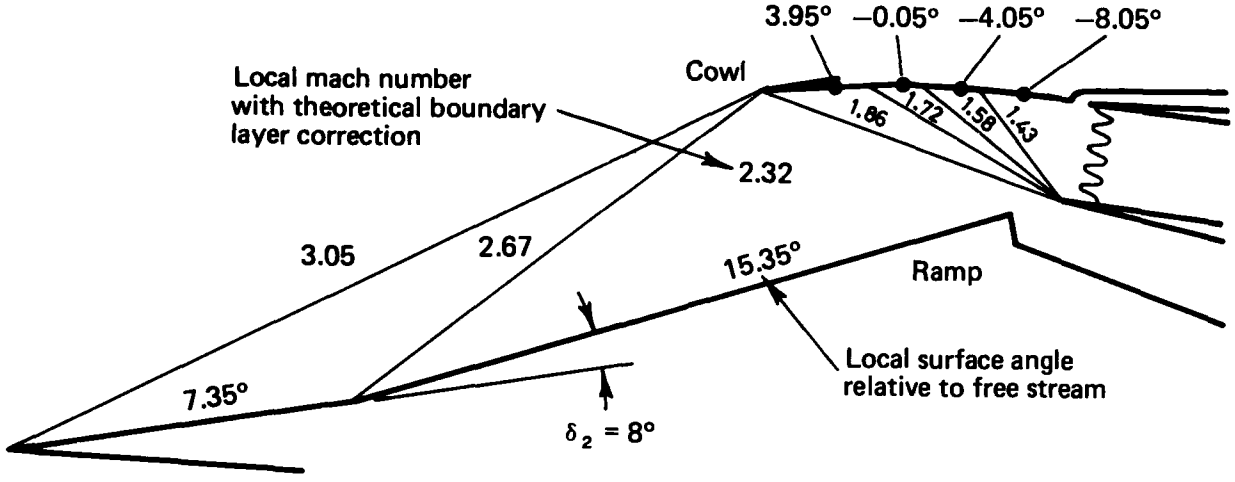

FIG. 2 SUPERSONIC DIFFUSER

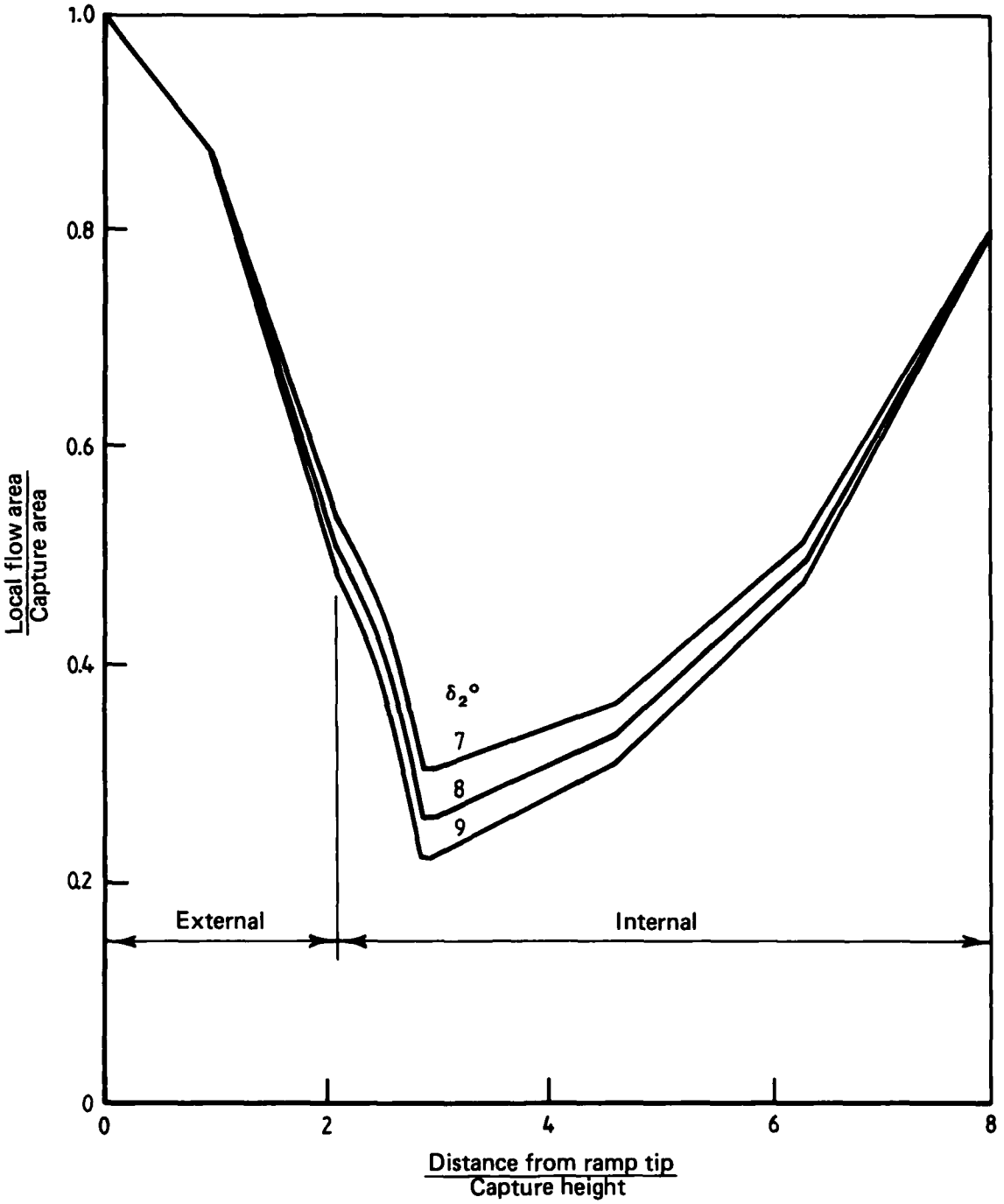

FIG. 3 FLOW AREA DISTRIBUTION

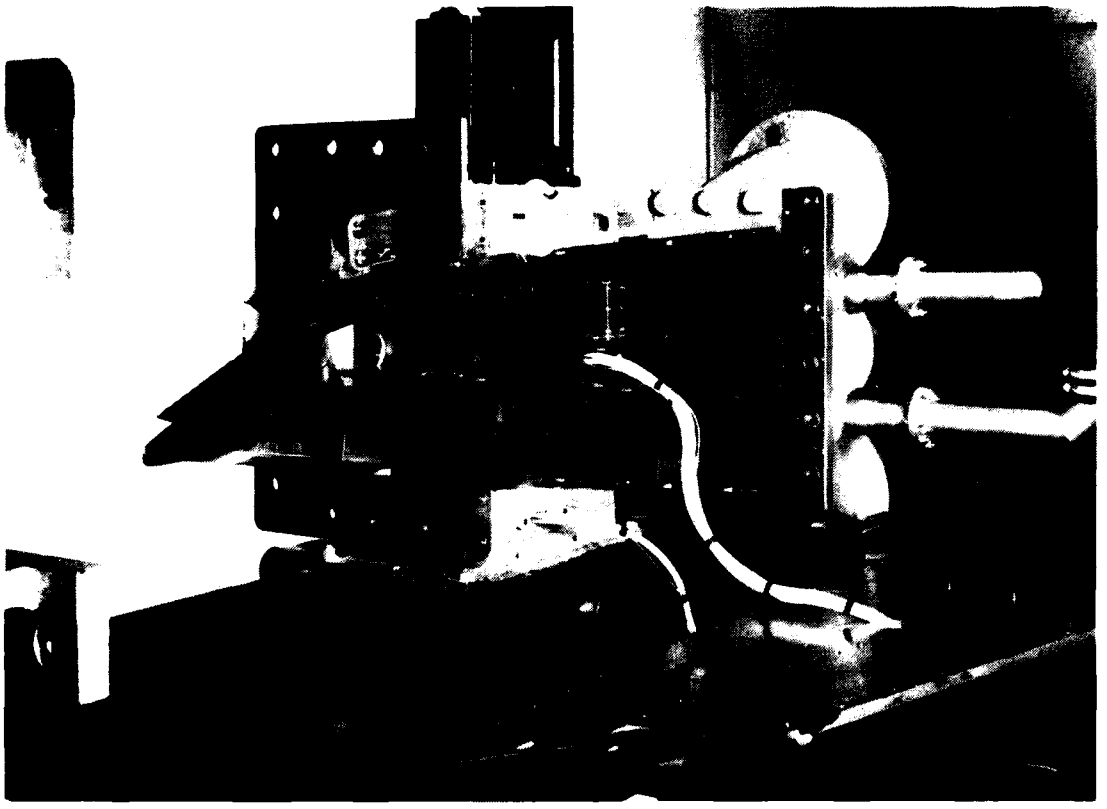

FIG. 4 SPILL DIFFUSER ARRANGEMENT

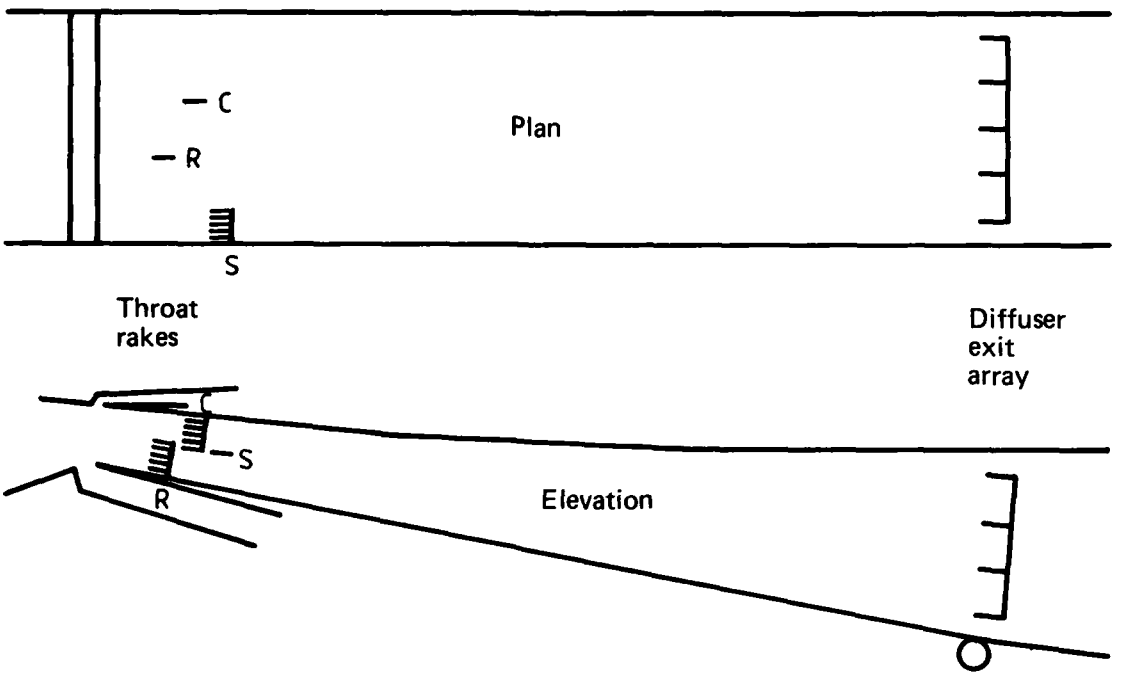

(a) Pitot probe locations

(b) Throat rakes

FIG. 5 SUBSONIC DIFFUSER INSTRUMENTATION

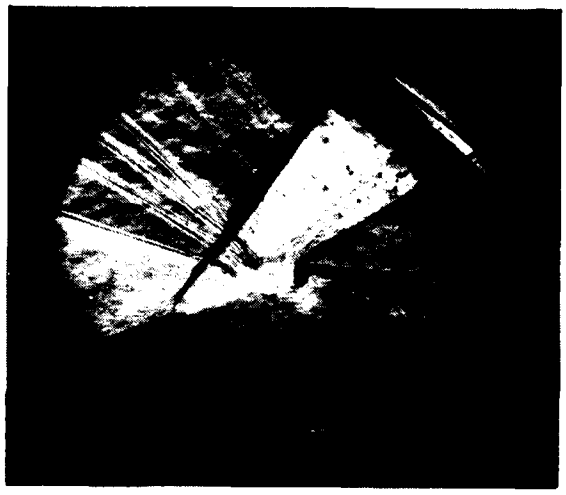

(a) Schlieren photograph

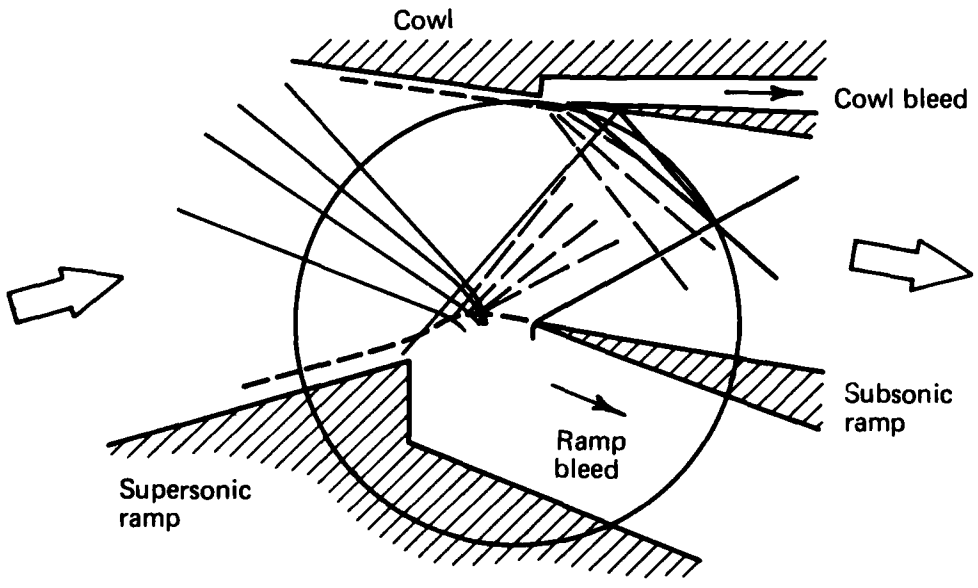

(b) Two-dimensional interpretation

FIG. 6 THROAT FLOW IN DATUM CONFIGURATION – $\delta_2 = 8°$, $t/H_i = 0$, SUPERCRITICAL

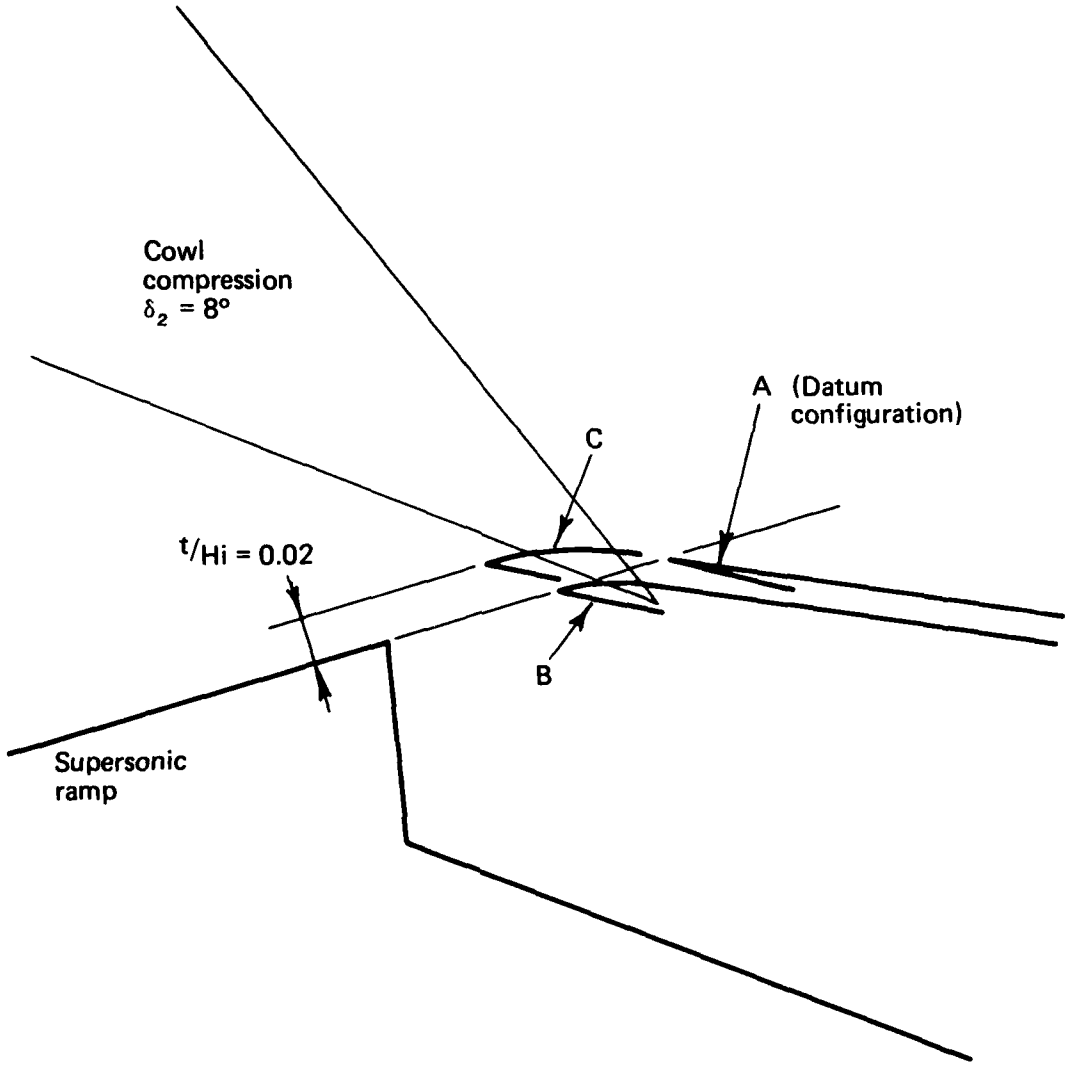

FIG. 7 RAMP BLEED SLOT VARIANTS

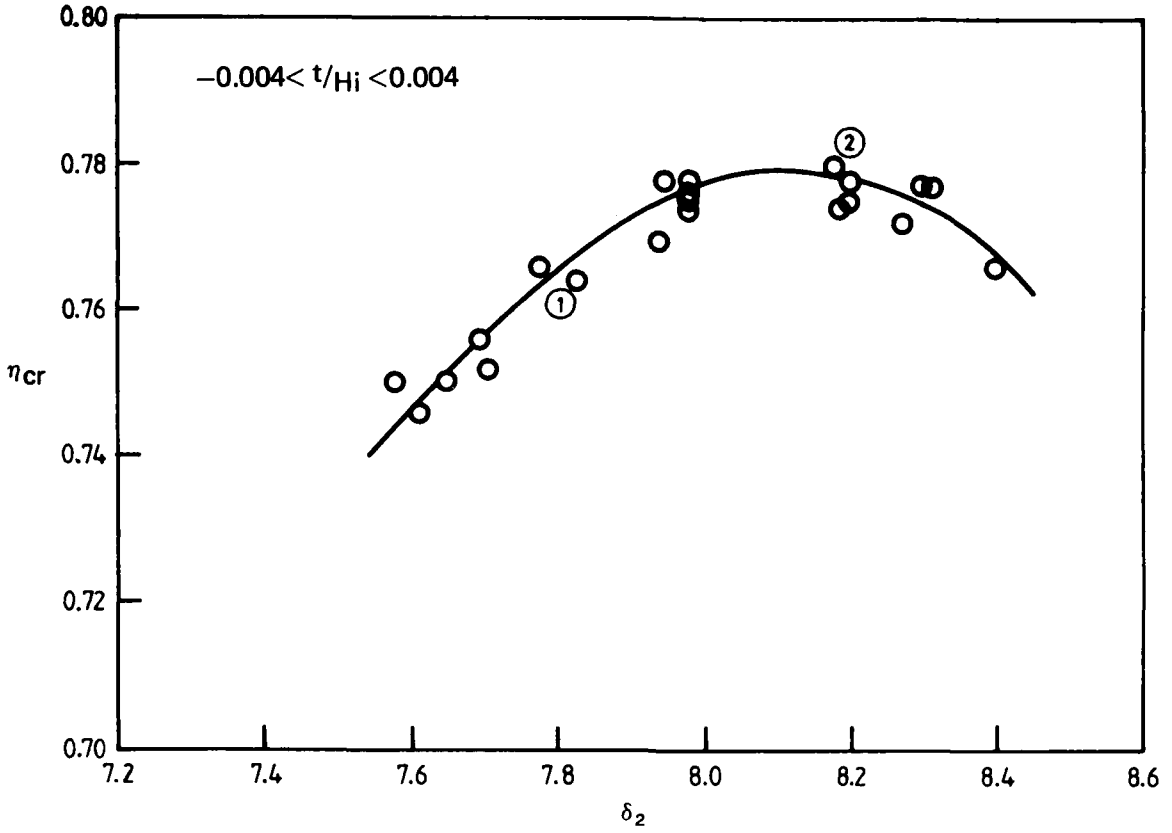

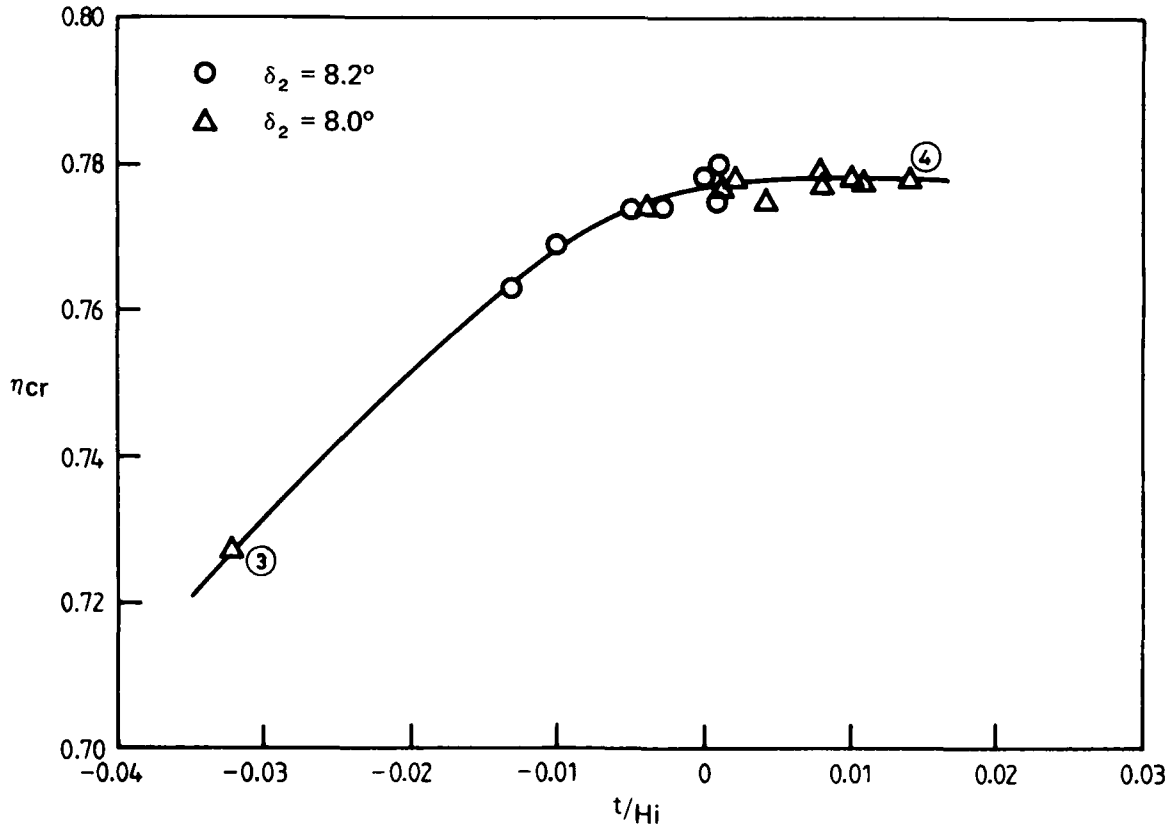

FIG. 8 EFFECT OF GEOMETRY ON PRESSURE RECOVERY – RAMP BLEED SLOT A

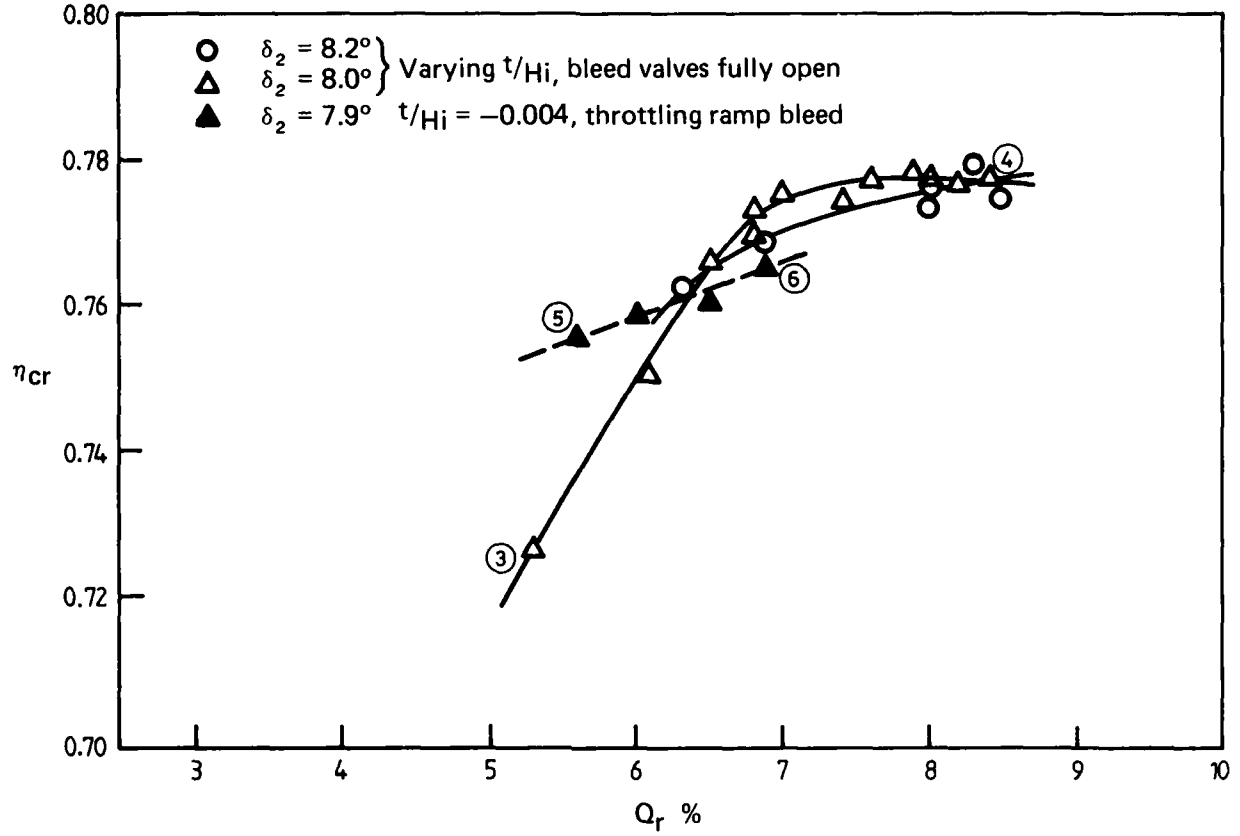

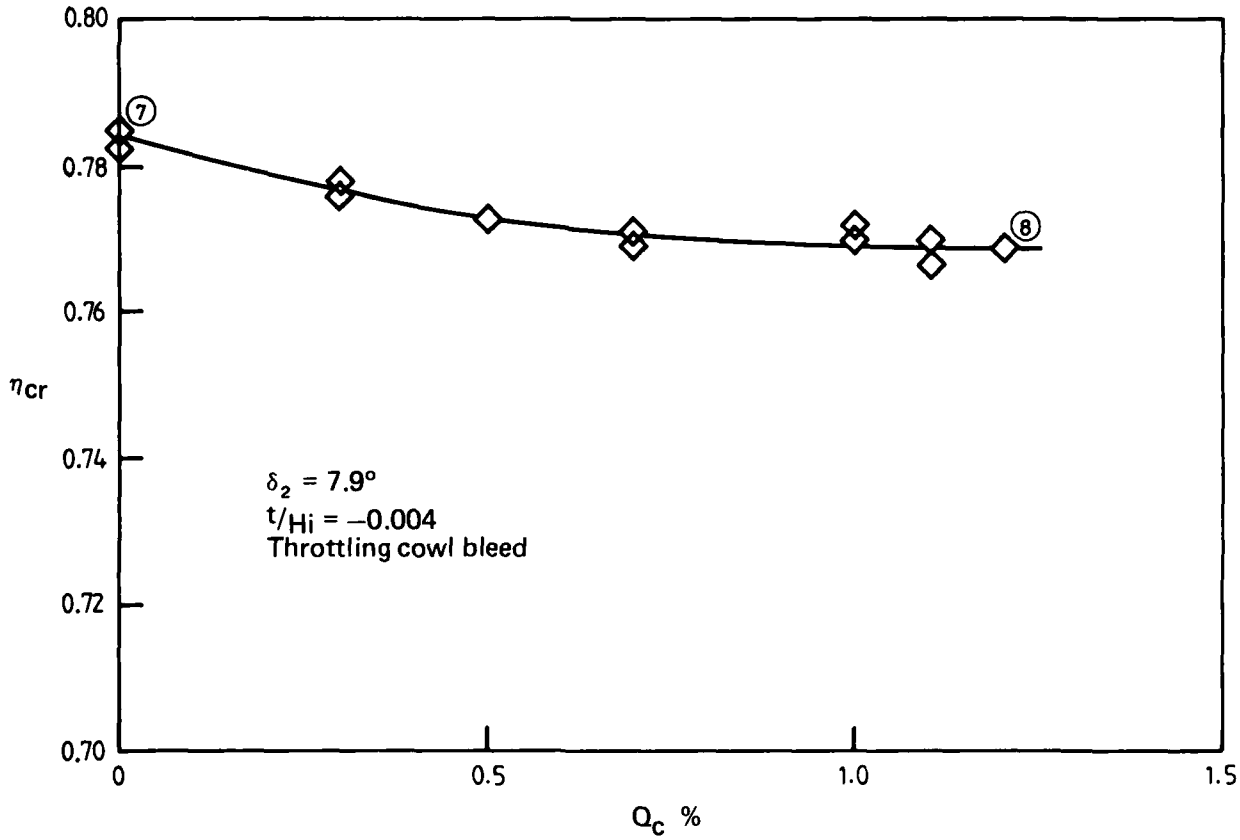

FIG. 9 EFFECT OF BLEED FLOW ON PRESSURE RECOVERY – RAMP BLEED SLOT A

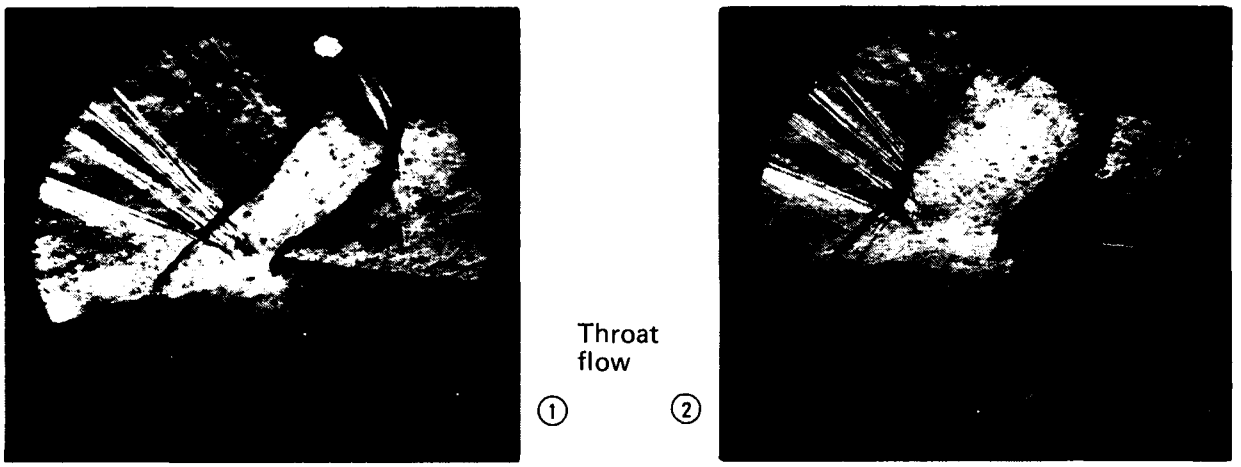

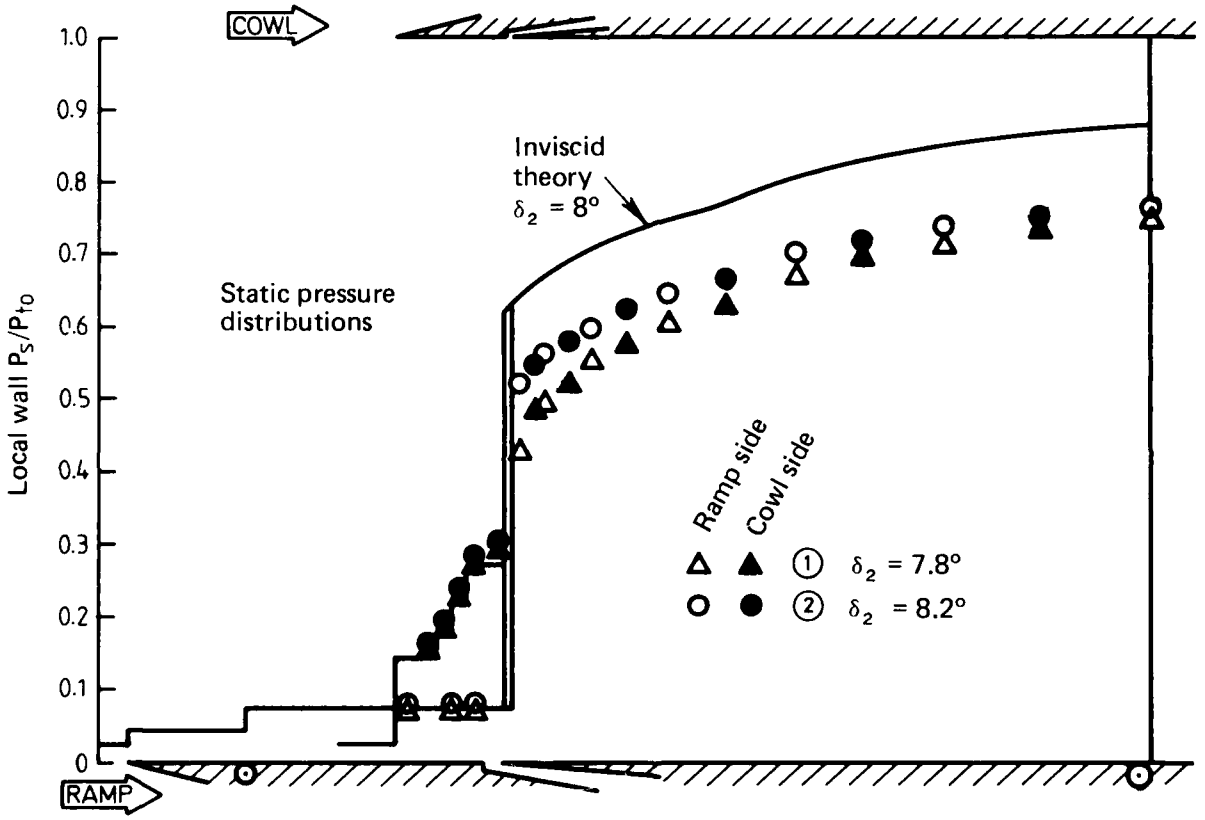

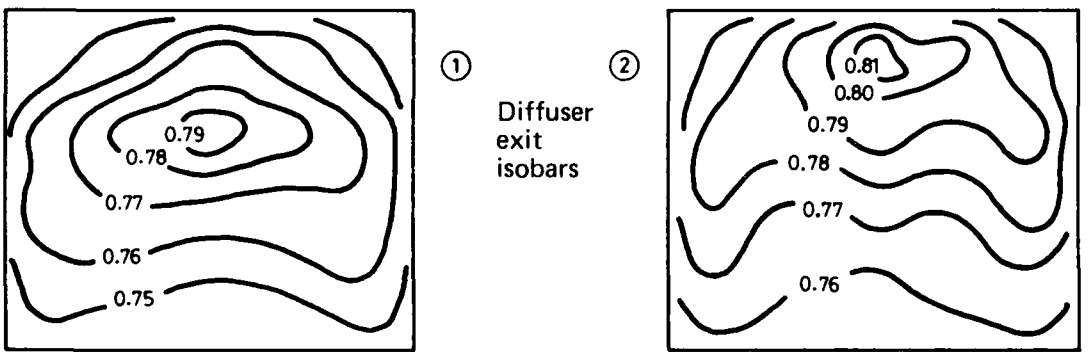

FIG. 10 EFFECT OF RAMP ANGLE – RAMP BLEED SLOT A, $-0.004 < {}^{t}/_{Hi} < +0.004$

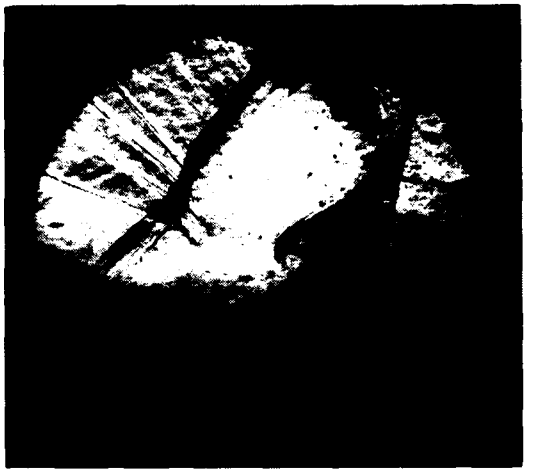

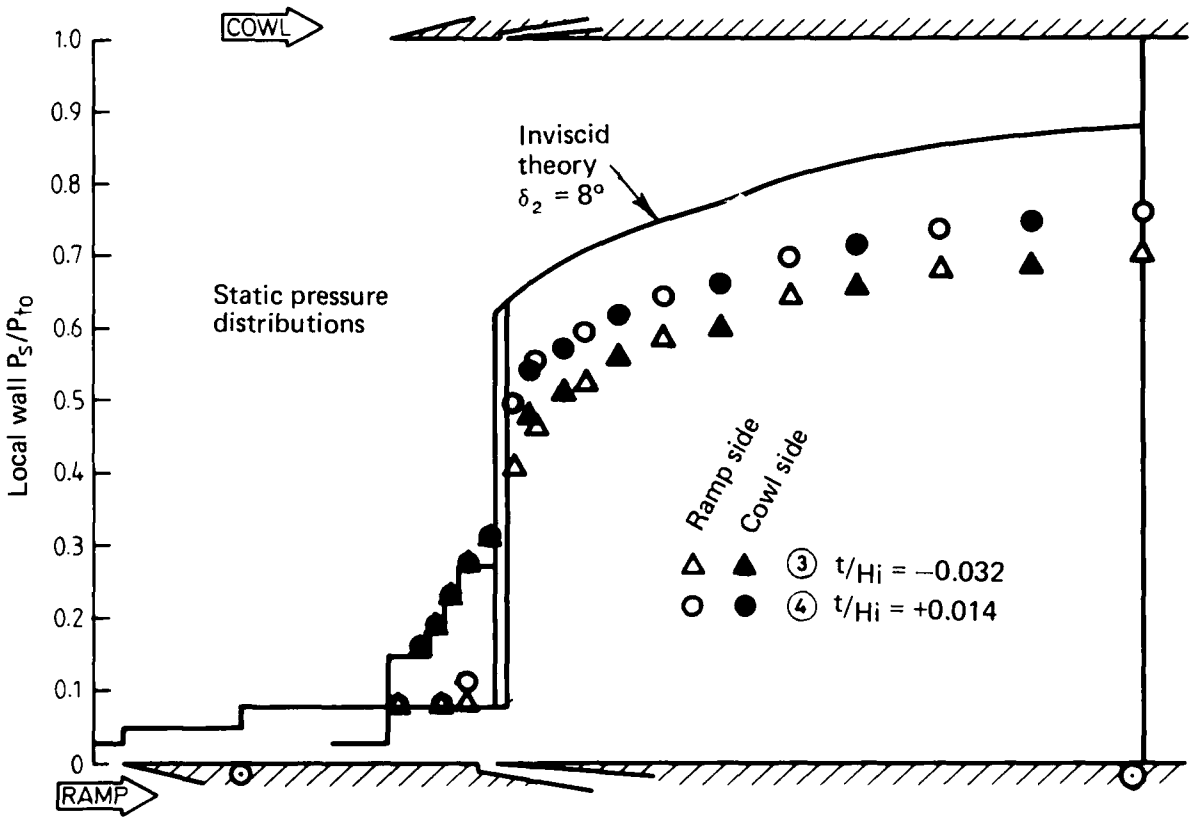

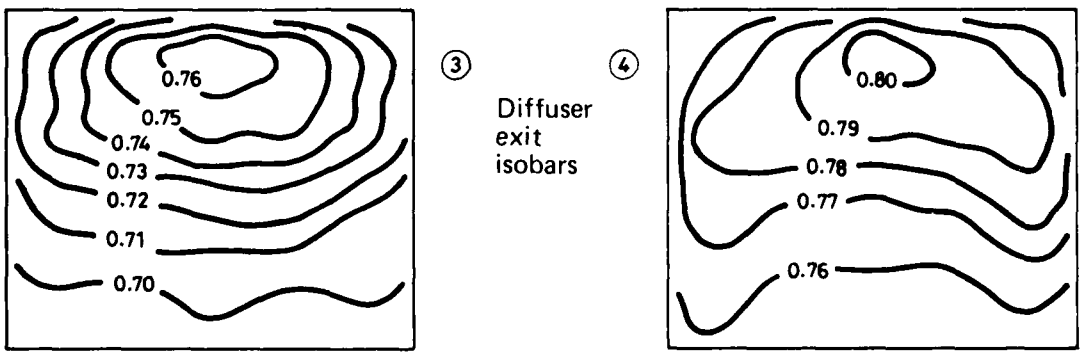

FIG. 11 EFFECT OF RAMP BLEED GEOMETRY – RAMP BLEED SLOT A, $\delta_2 = 8°$

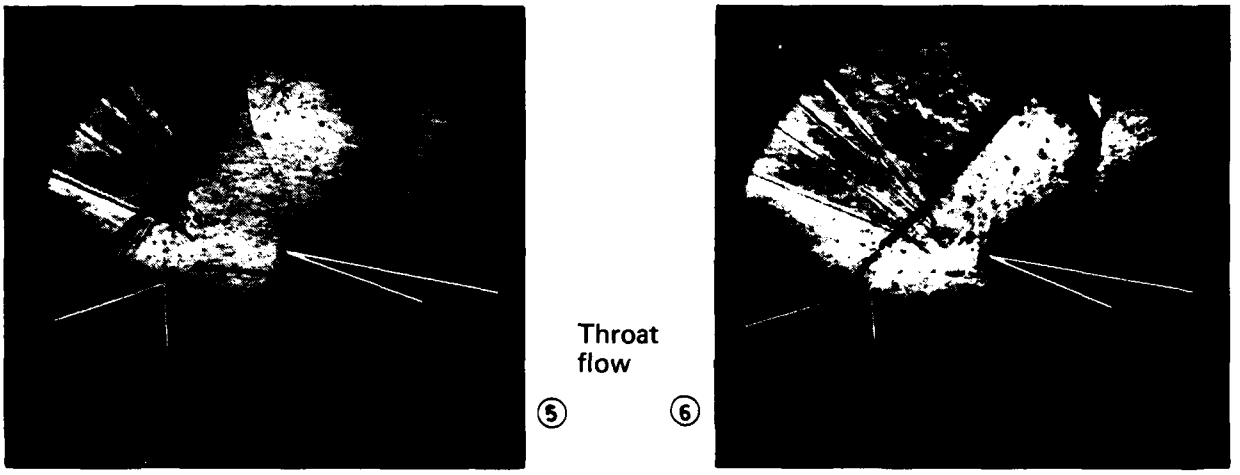

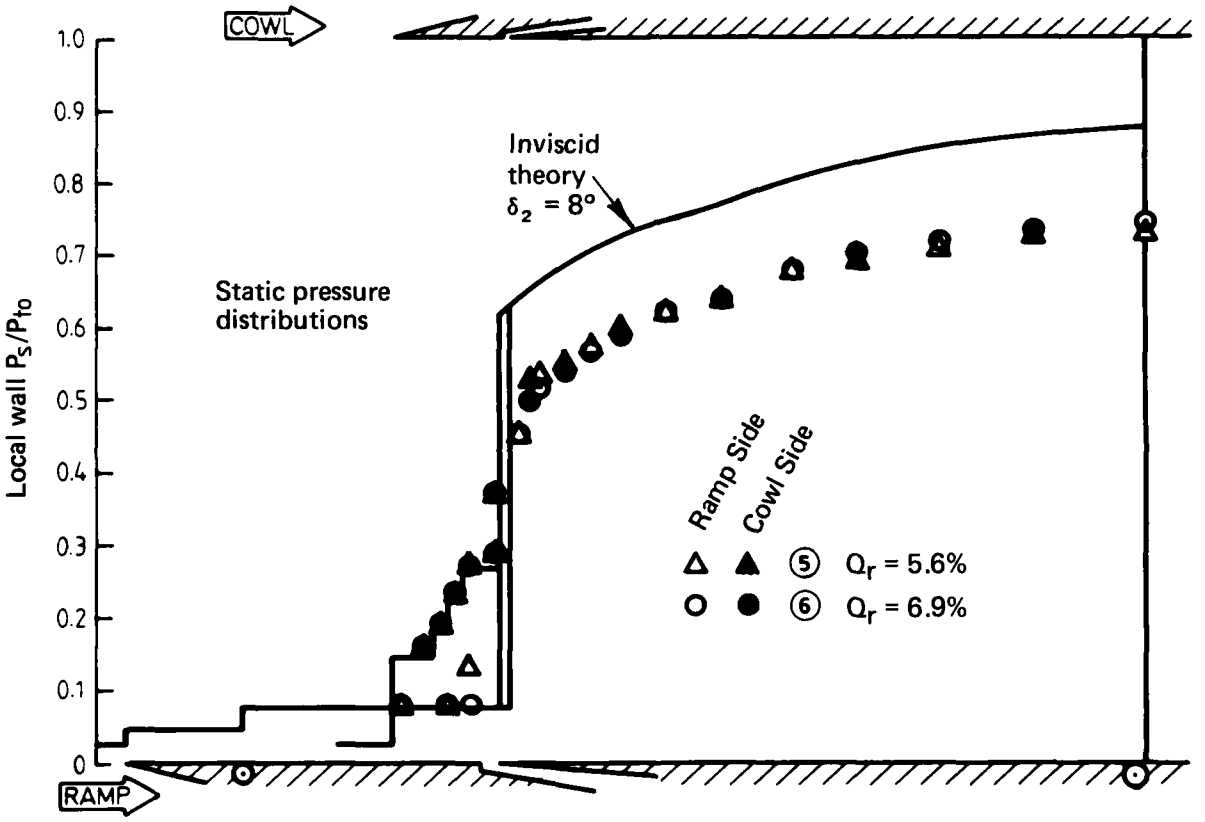

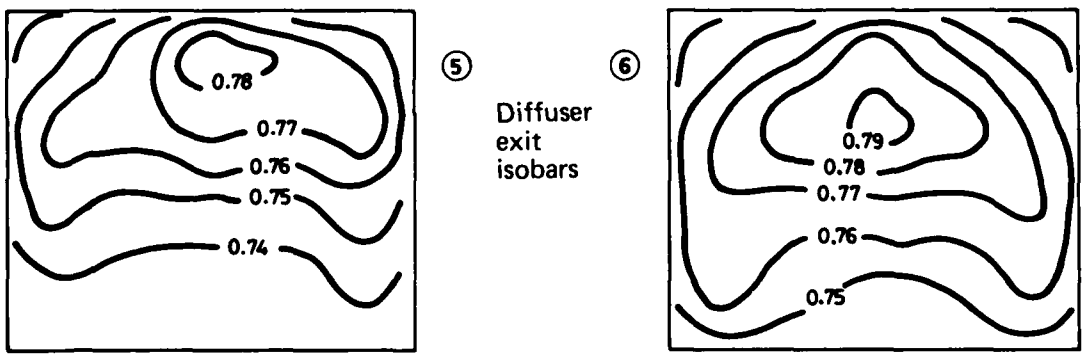

FIG. 12 EFFECT OF THROTTLING RAMP BLEED – RAMP BLEED SLOT A, $\delta_2 = 7.9°$, $t/_{Hi} = -0.004$

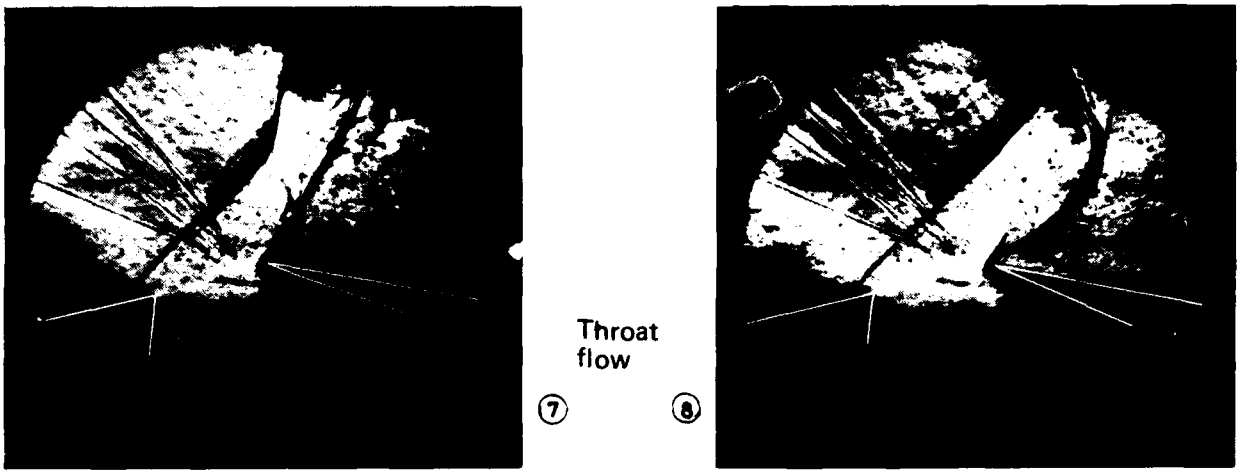

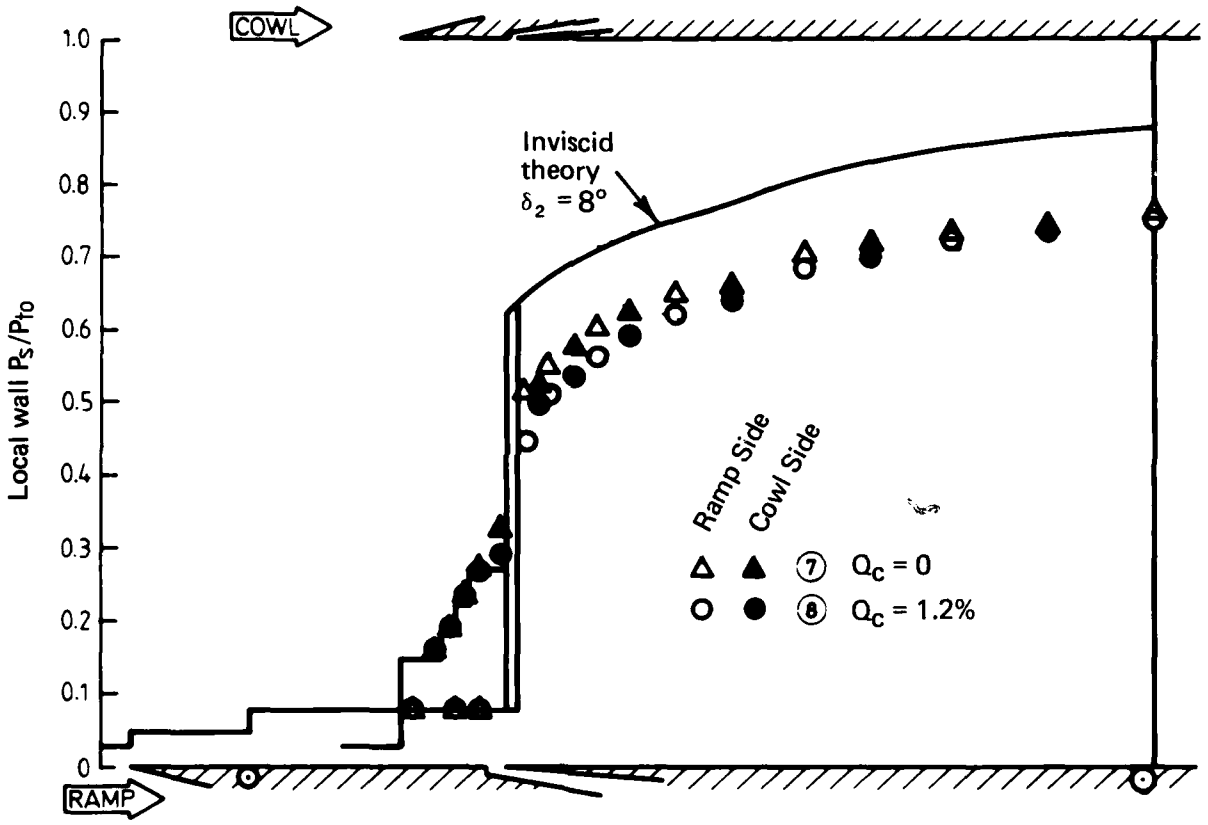

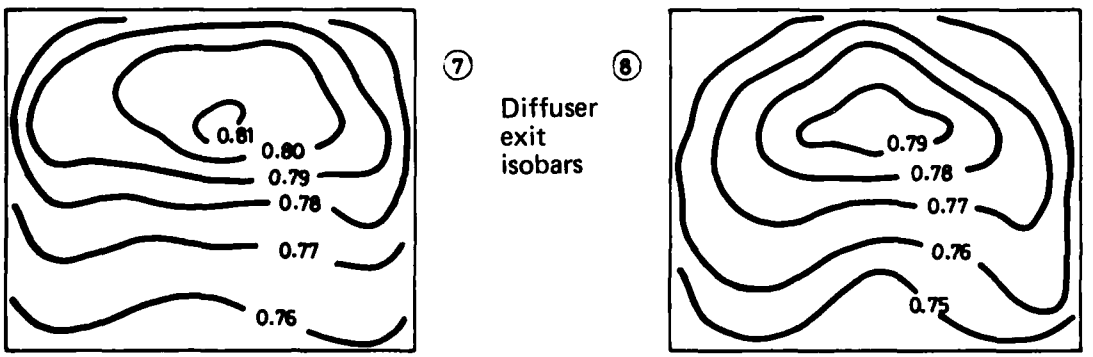

FIG. 13 EFFECT OF THROTTLING COWL BLEED – RAMP BLEED SLOT A, $\delta_2 = 7.9°$, $t/H_i = -0.004$

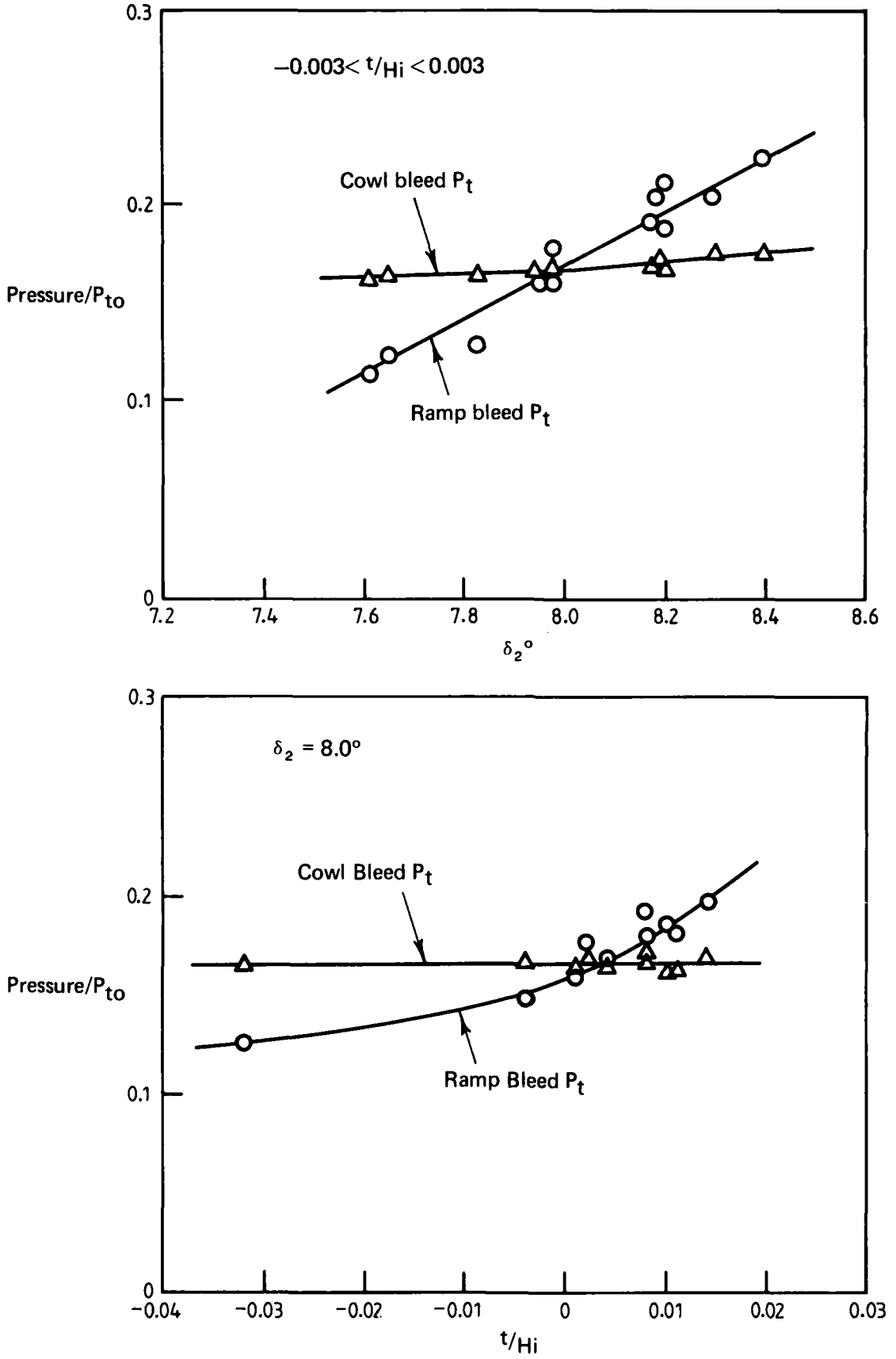

FIG. 14 BLEED PRESSURE RECOVERY – RAMP BLEED SLOT A

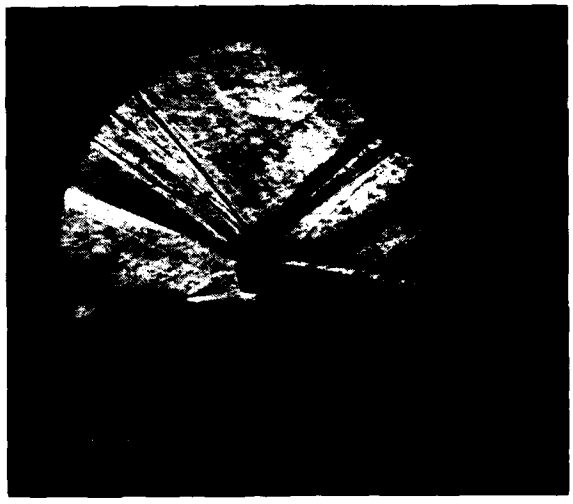

FIG. 15 THROAT FLOW IN CONFIGURATION B – δ_2 = 8°, t/H_i = 0, SUPERCRITICAL

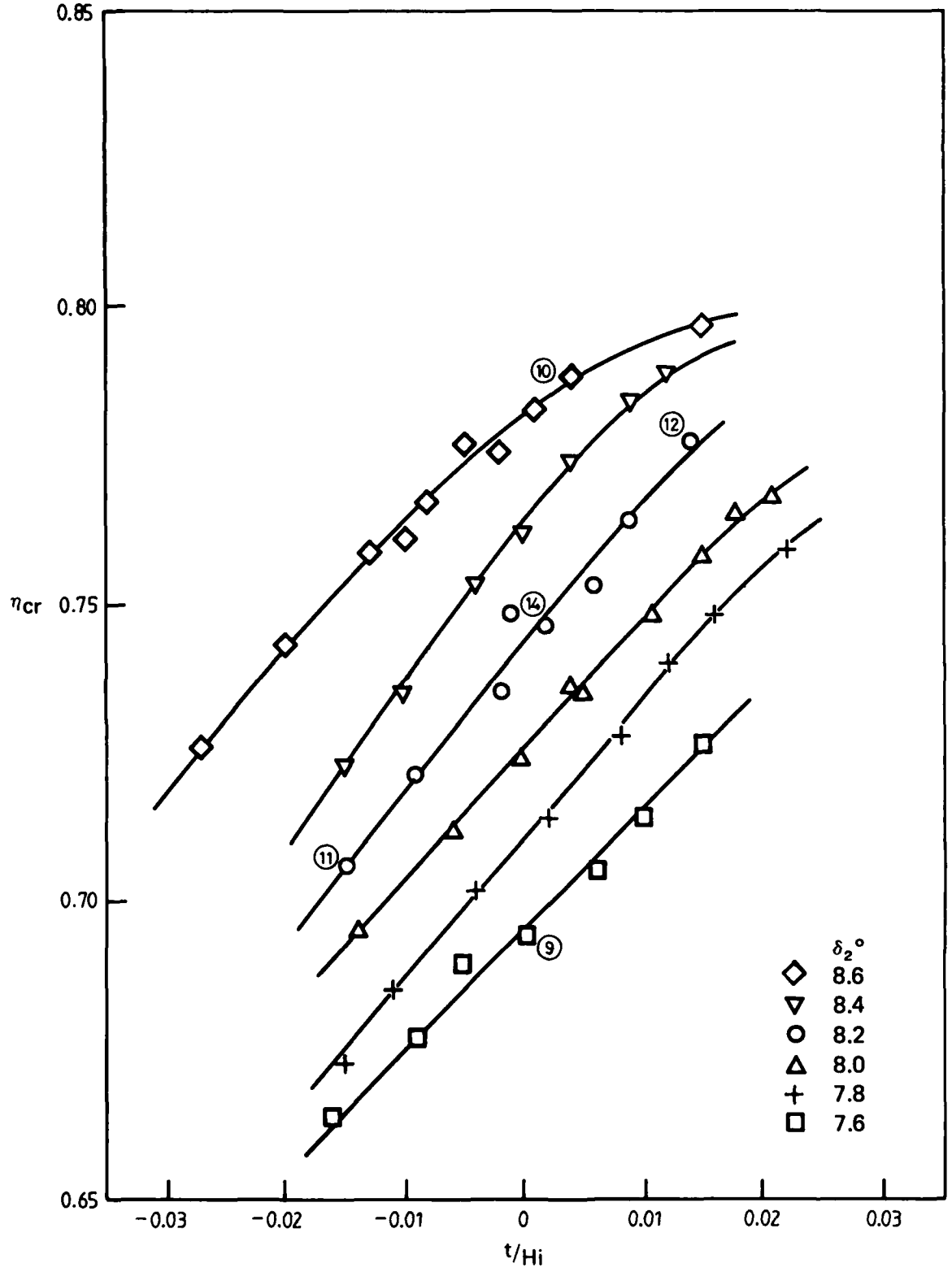

FIG. 16 EFFECT OF GEOMETRY ON PRESSURE RECOVERY – RAMP BLEED SLOT B

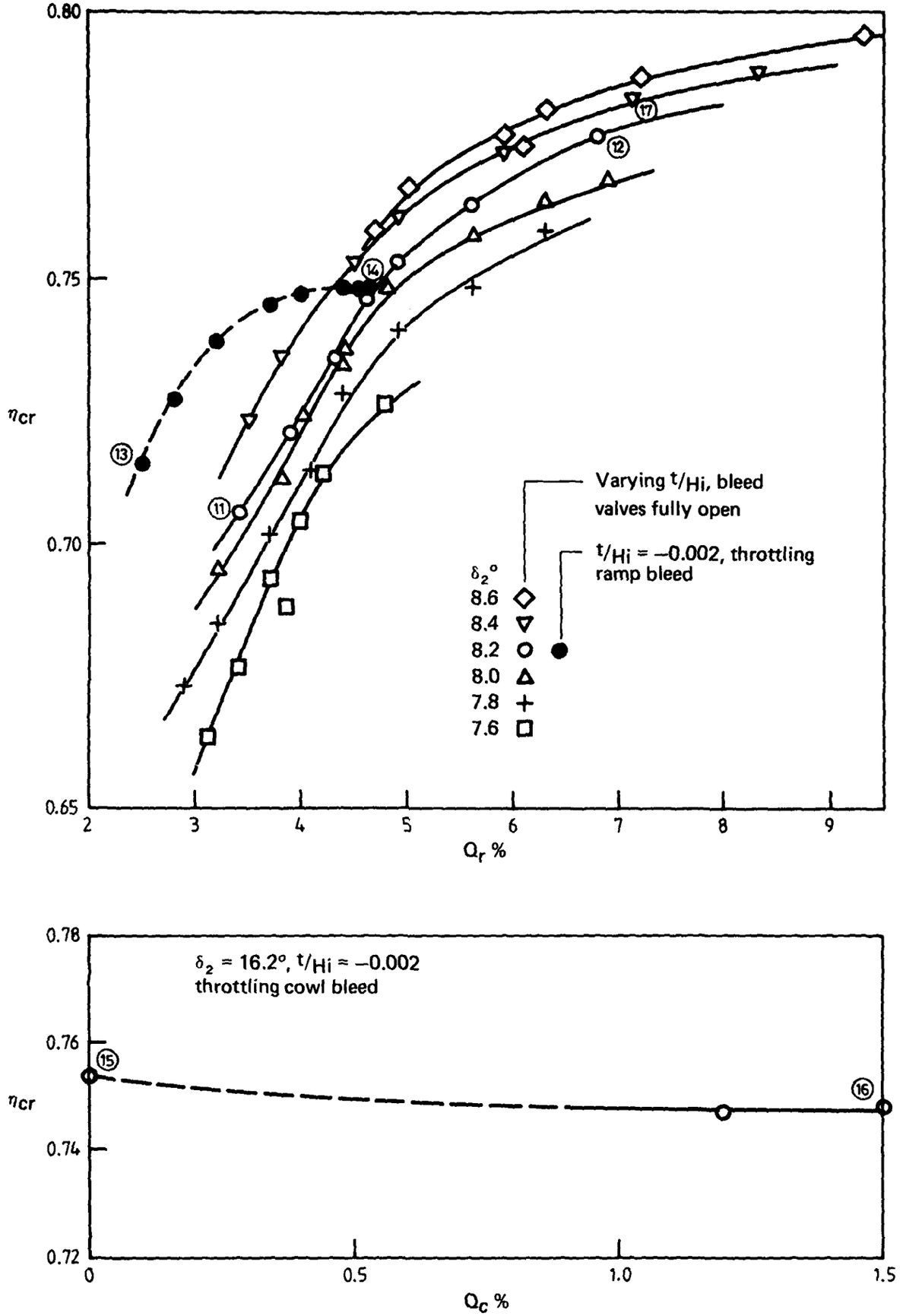

FIG. 17 EFFECT OF BLEED FLOW ON PRESSURE RECOVERY – RAMP BLEED SLOT B

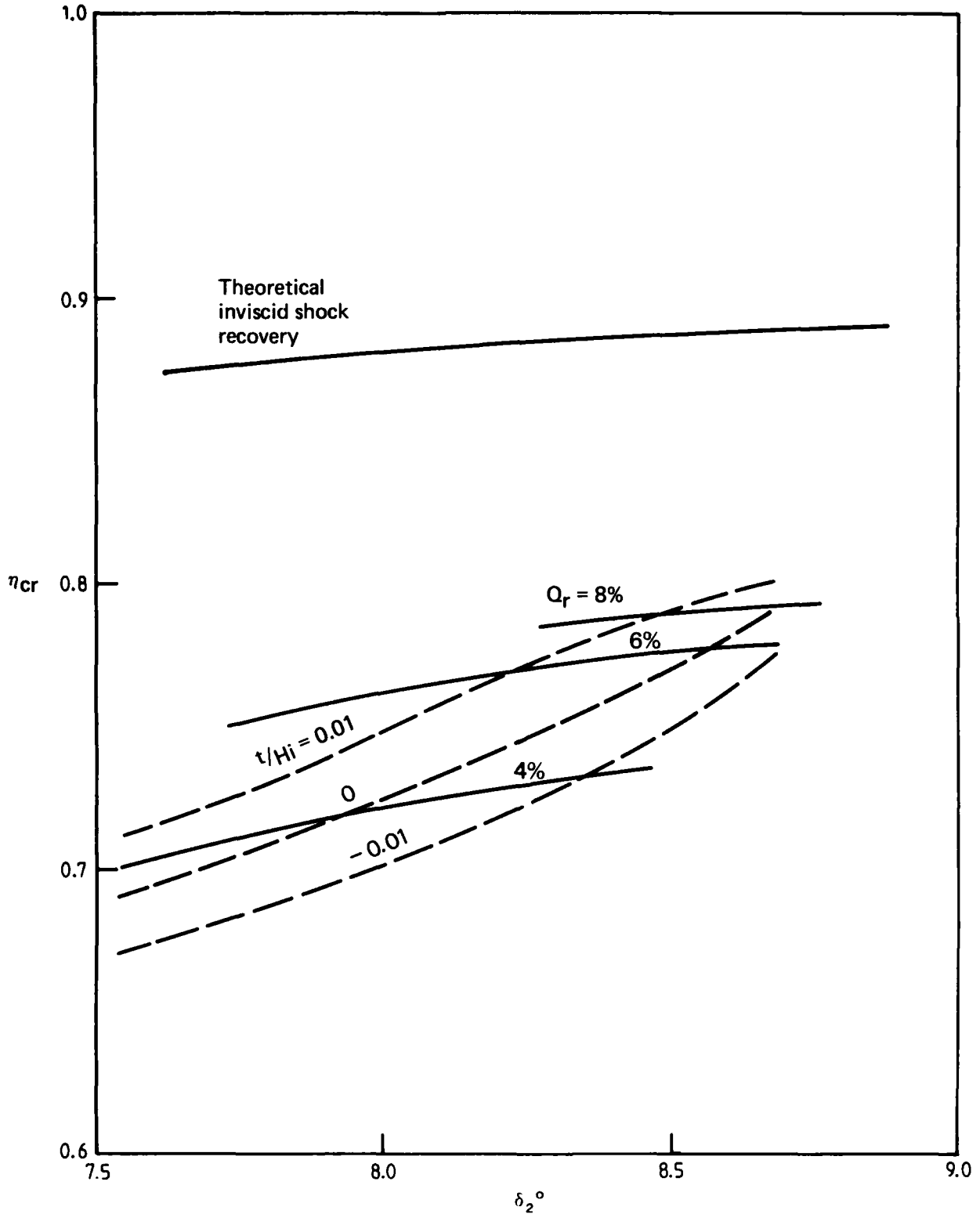

FIG. 18 MEASURED PRESSURE RECOVERY COMPARED WITH THEORETICAL SHOCK RECOVERY – RAMP BLEED SLOT B

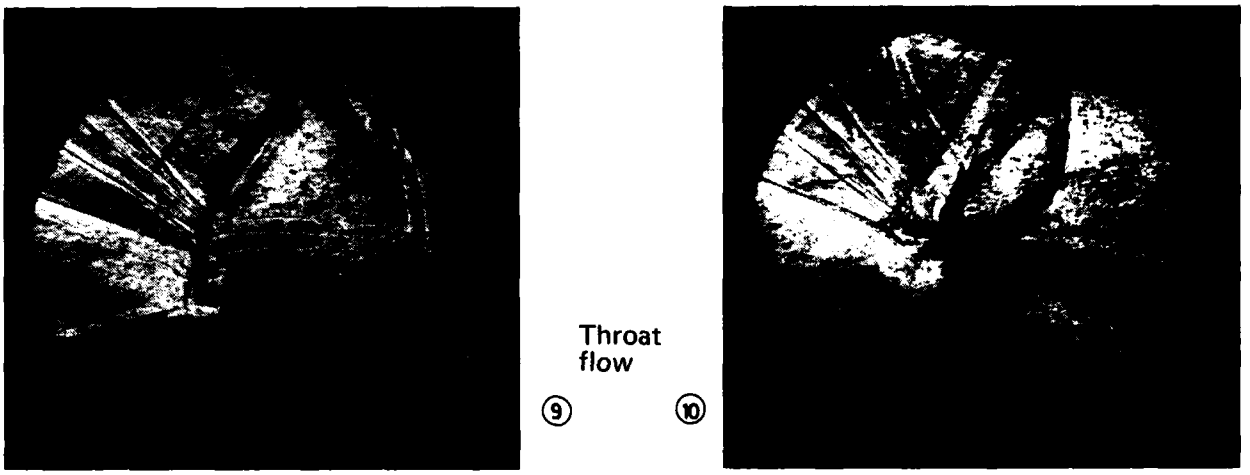

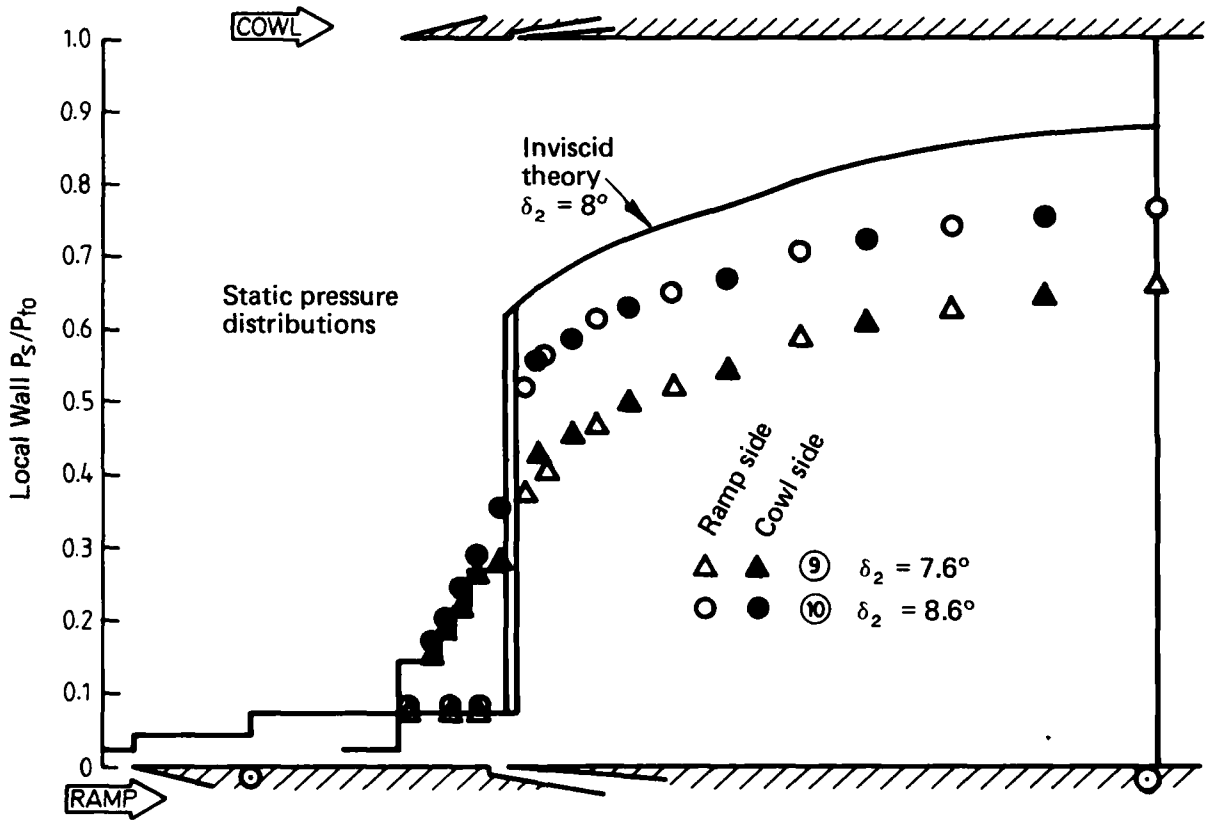

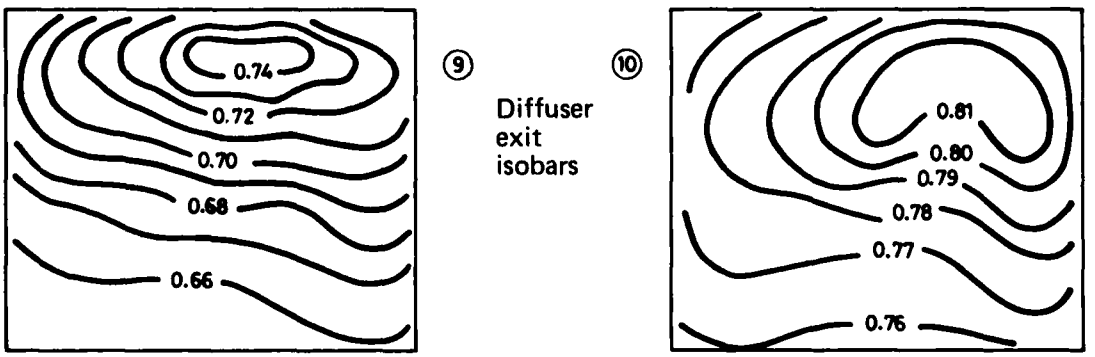

FIG. 19 EFFECT OF RAMP ANGLE – RAMP BLEED SLOT B, $0 < t/H_i < 0.004$

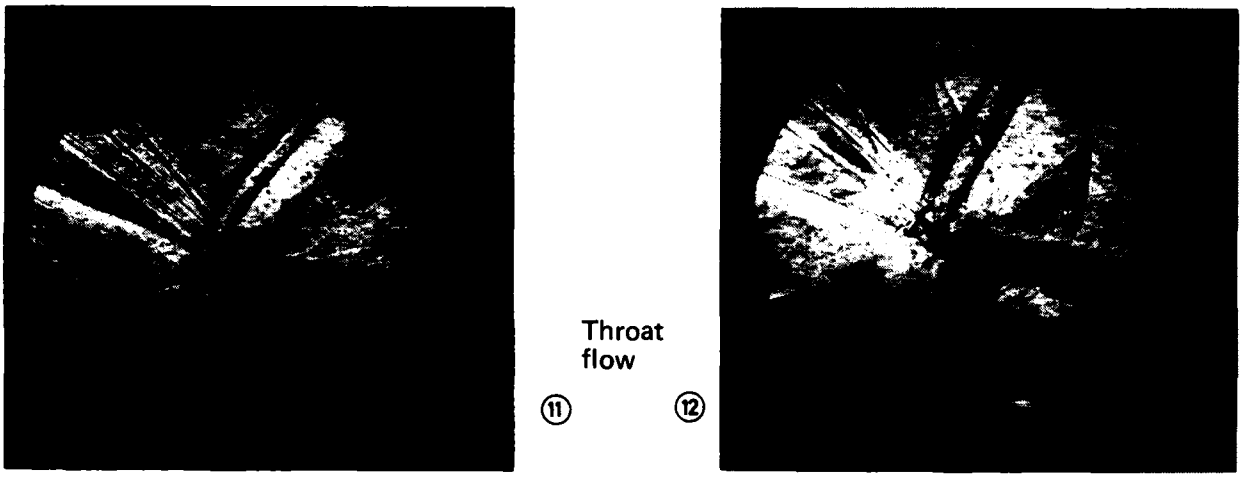

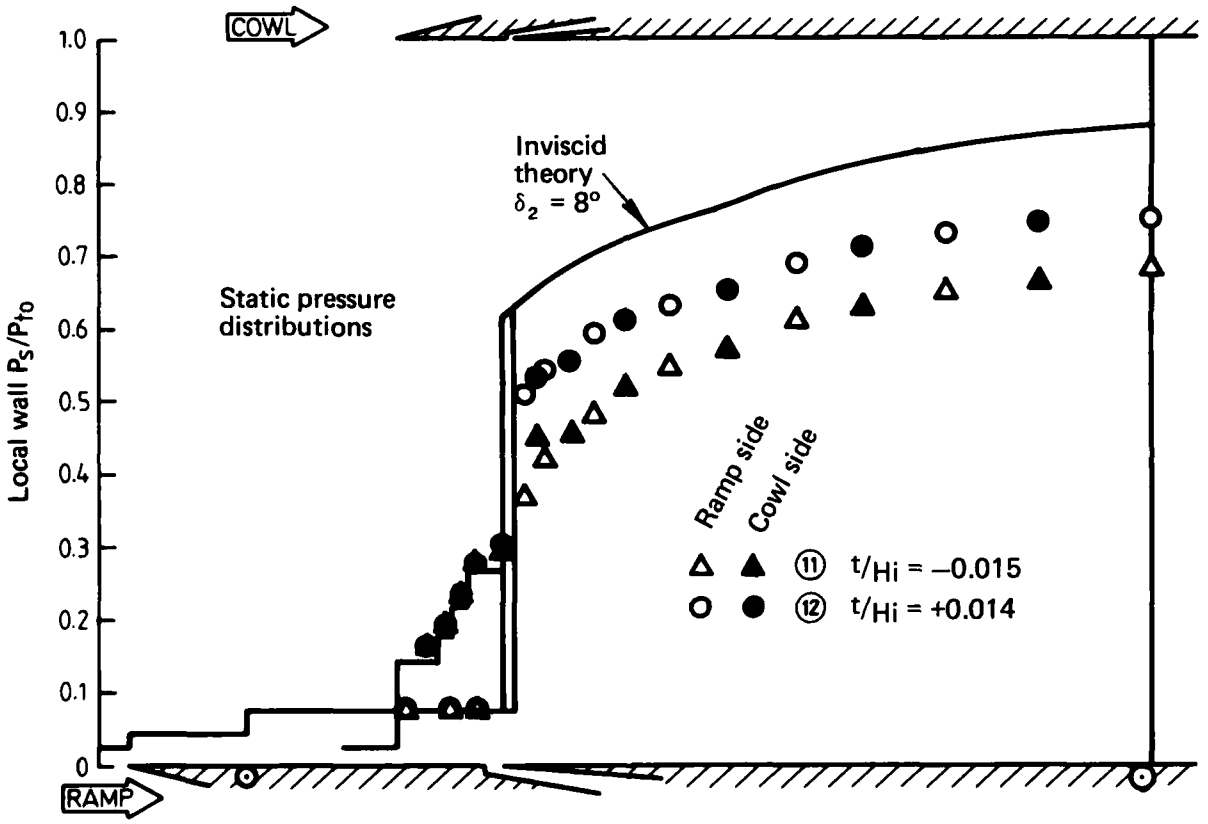

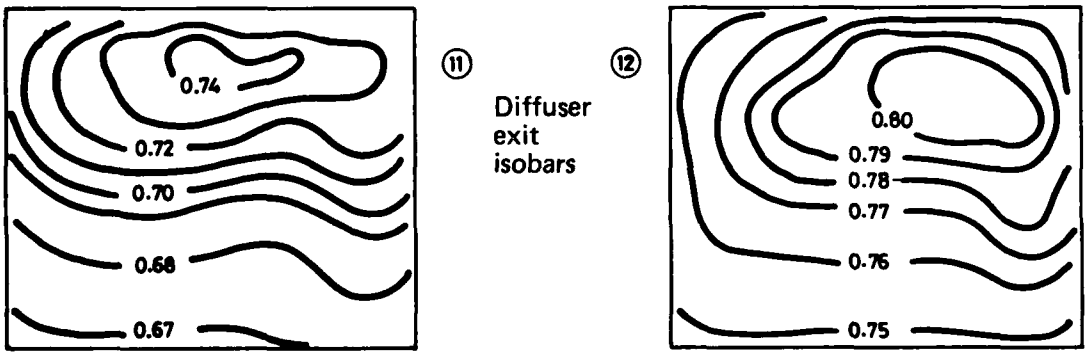

FIG. 20 EFFECT OF RAMP BLEED GEOMETRY – RAMP BLEED SLOT B, $\delta_2 = 8.2°$

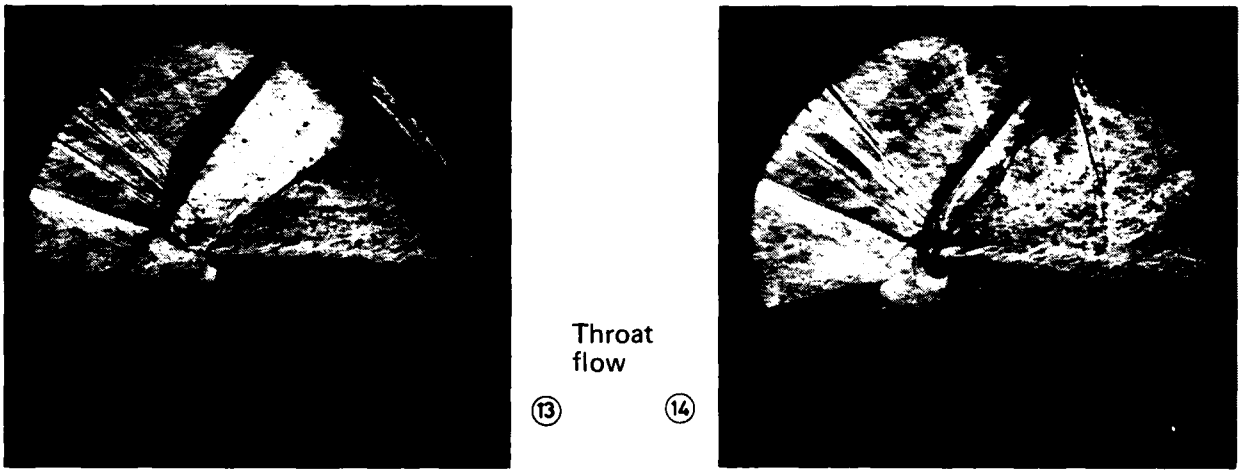

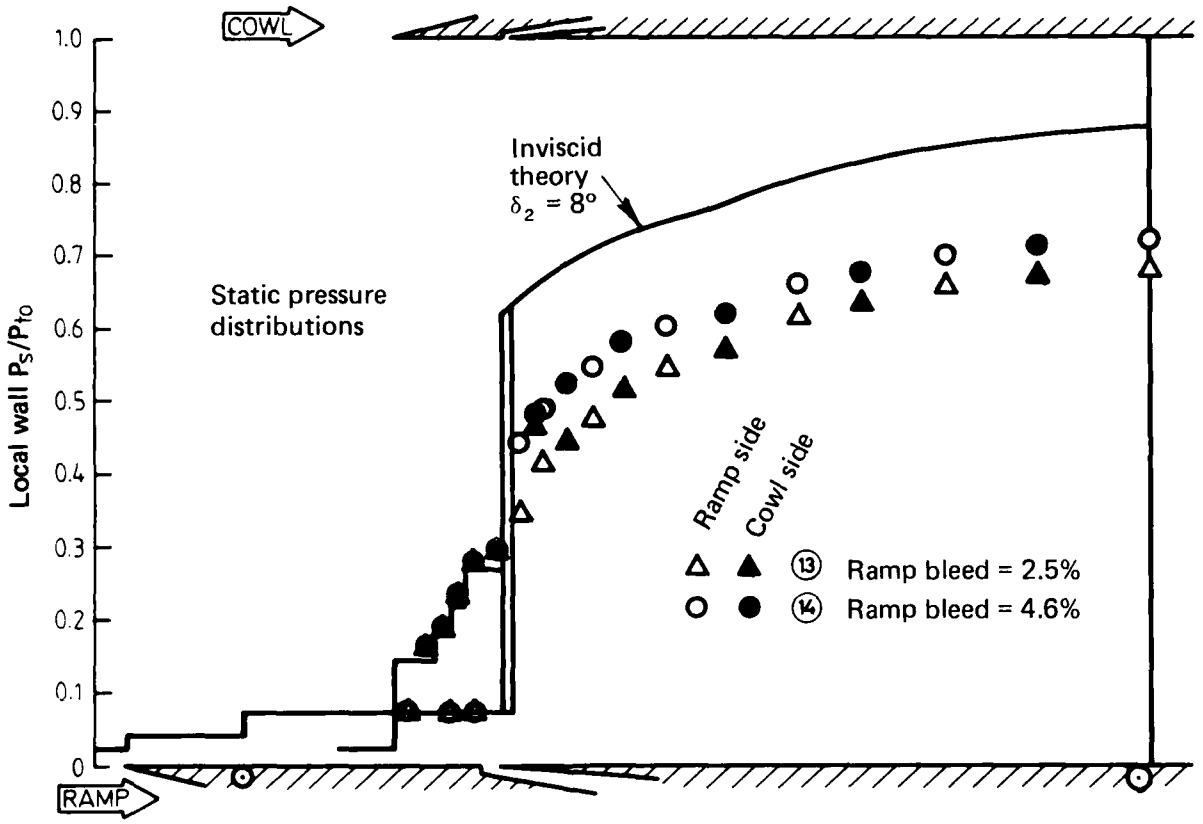

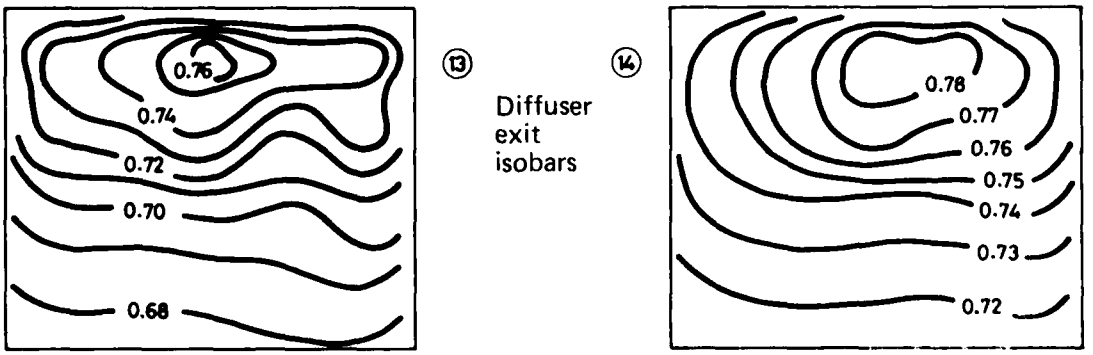

FIG. 21 EFFECT OF THROTTLING RAMP BLEED – RAMP BLEED SLOT B, $\delta_2 = 8.2°$, $t/_{Hi} = -0.002$

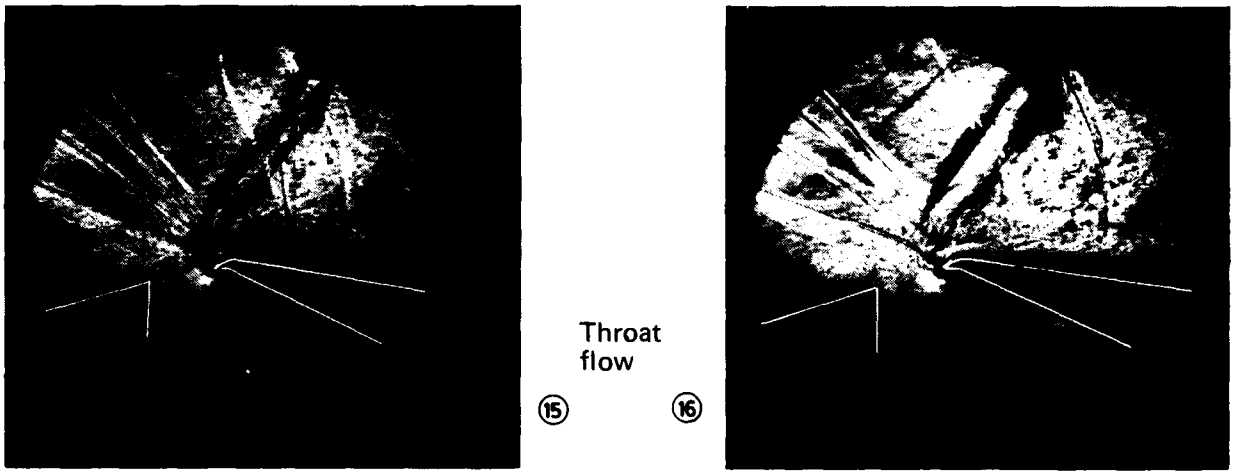

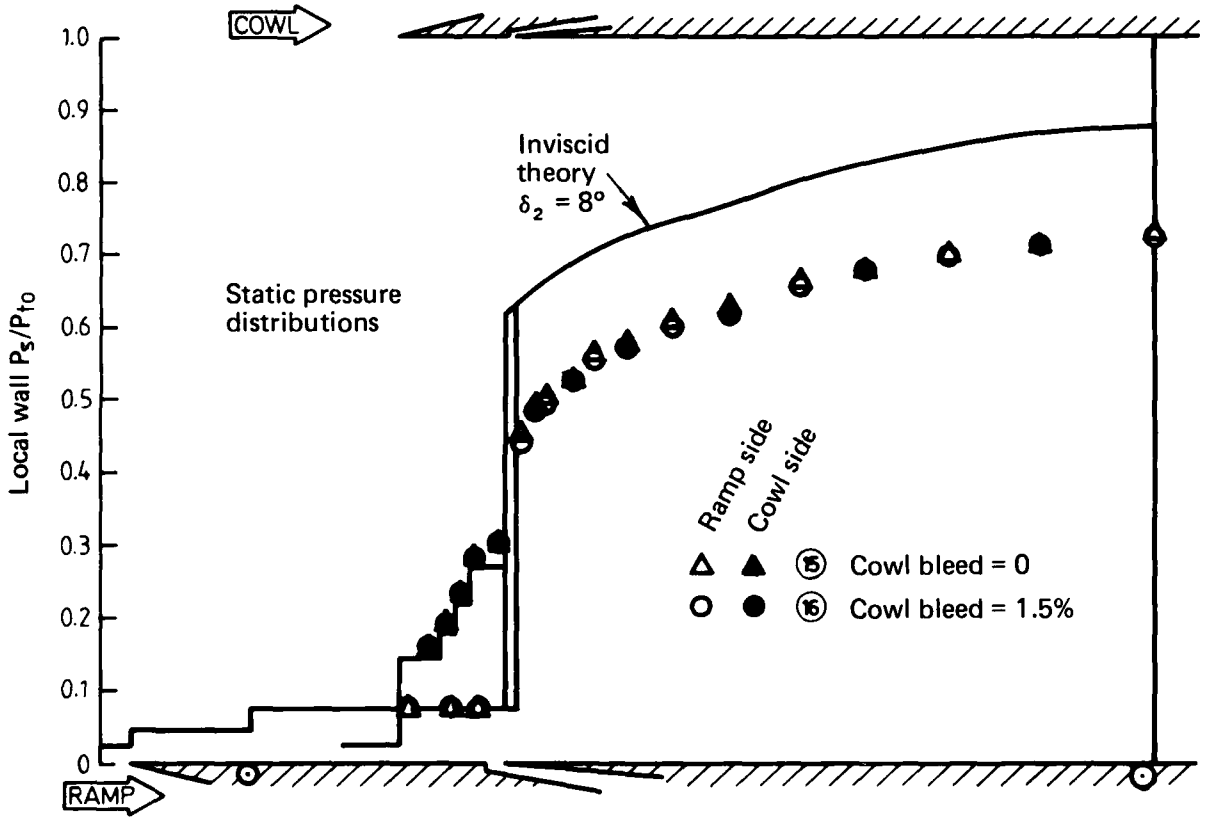

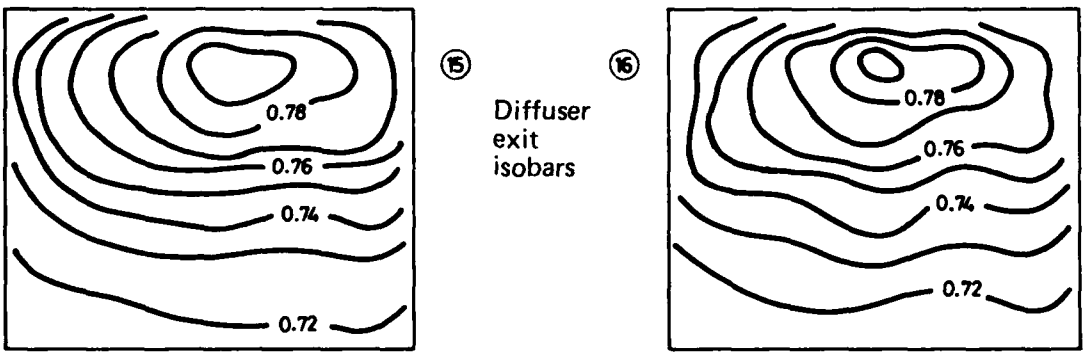

FIG. 22 EFFECT OF COWL BLEED FLOW – RAMP BLEED SLOT B,
$\delta_2 = 8.2°$, $t/H_i = -0.002$

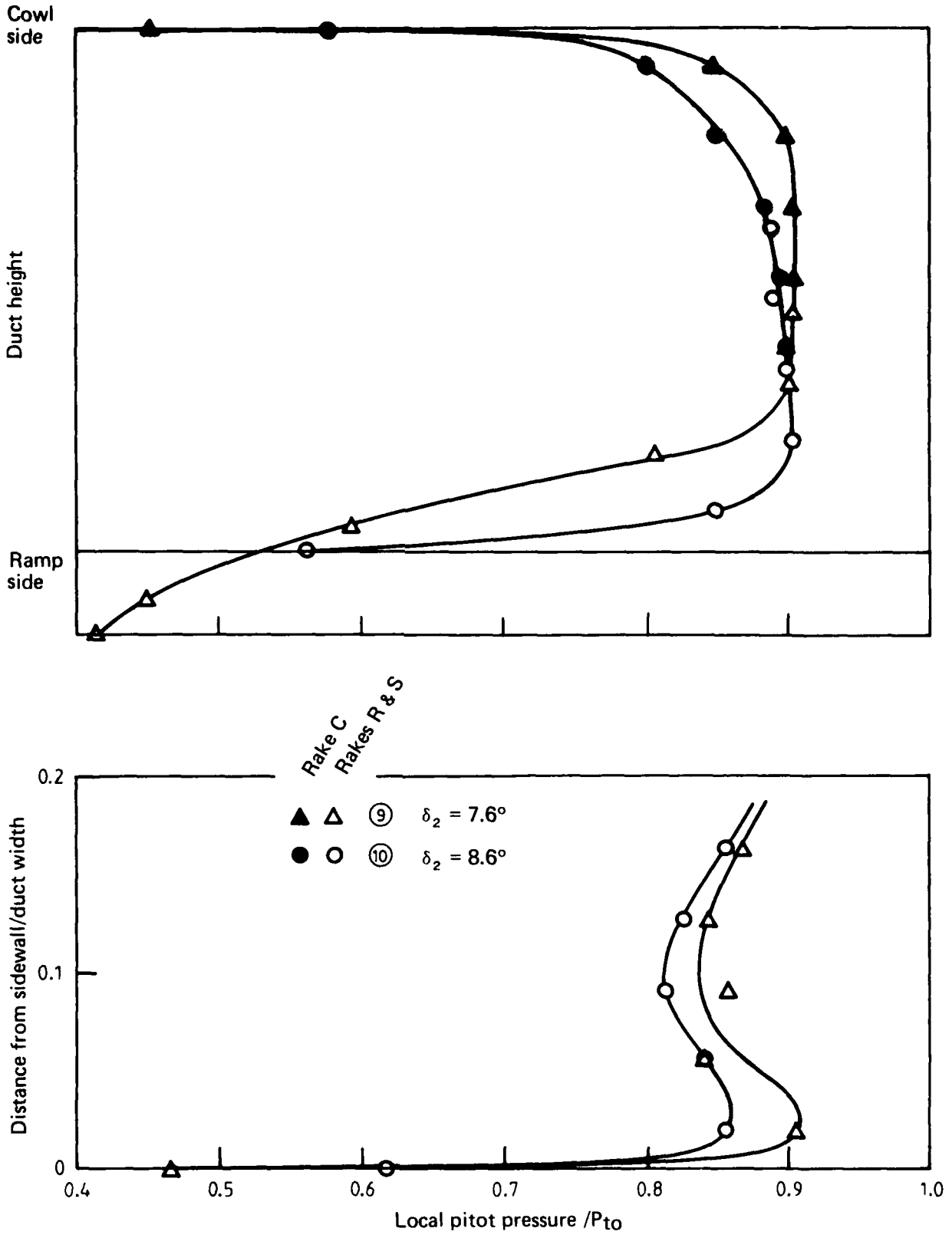

FIG. 23 EFFECT OF RAMP ANGLE ON THROAT FLOW PROFILES – RAMP BLEED SLOT B, $0 < {}^{t}/_{H_i} < 0.004$

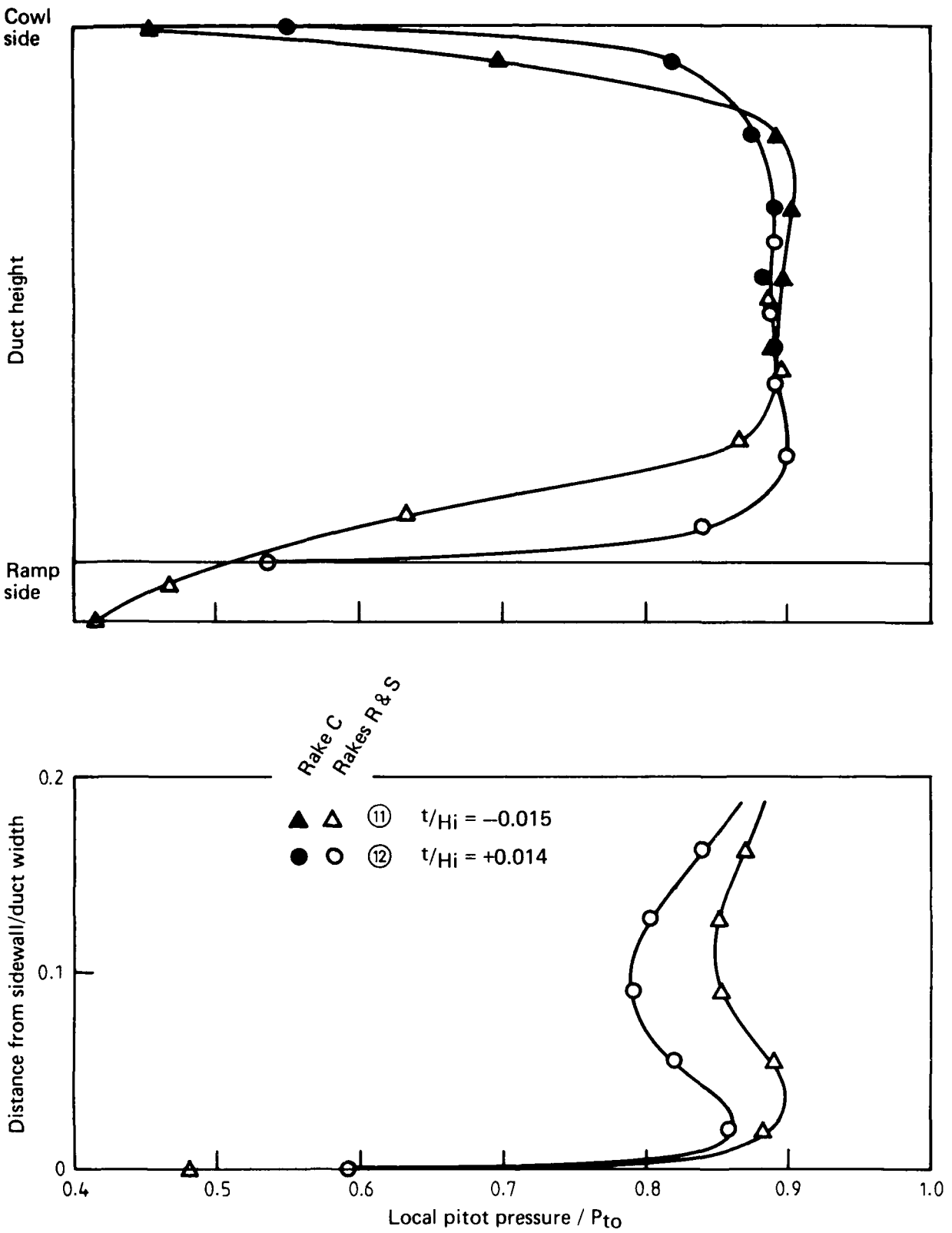

FIG. 24 EFFECT OF RAMP BLEED GEOMETRY ON THROAT FLOW PROFILES – RAMP BLEED SLOT B, $\delta_2 = 8.2°$

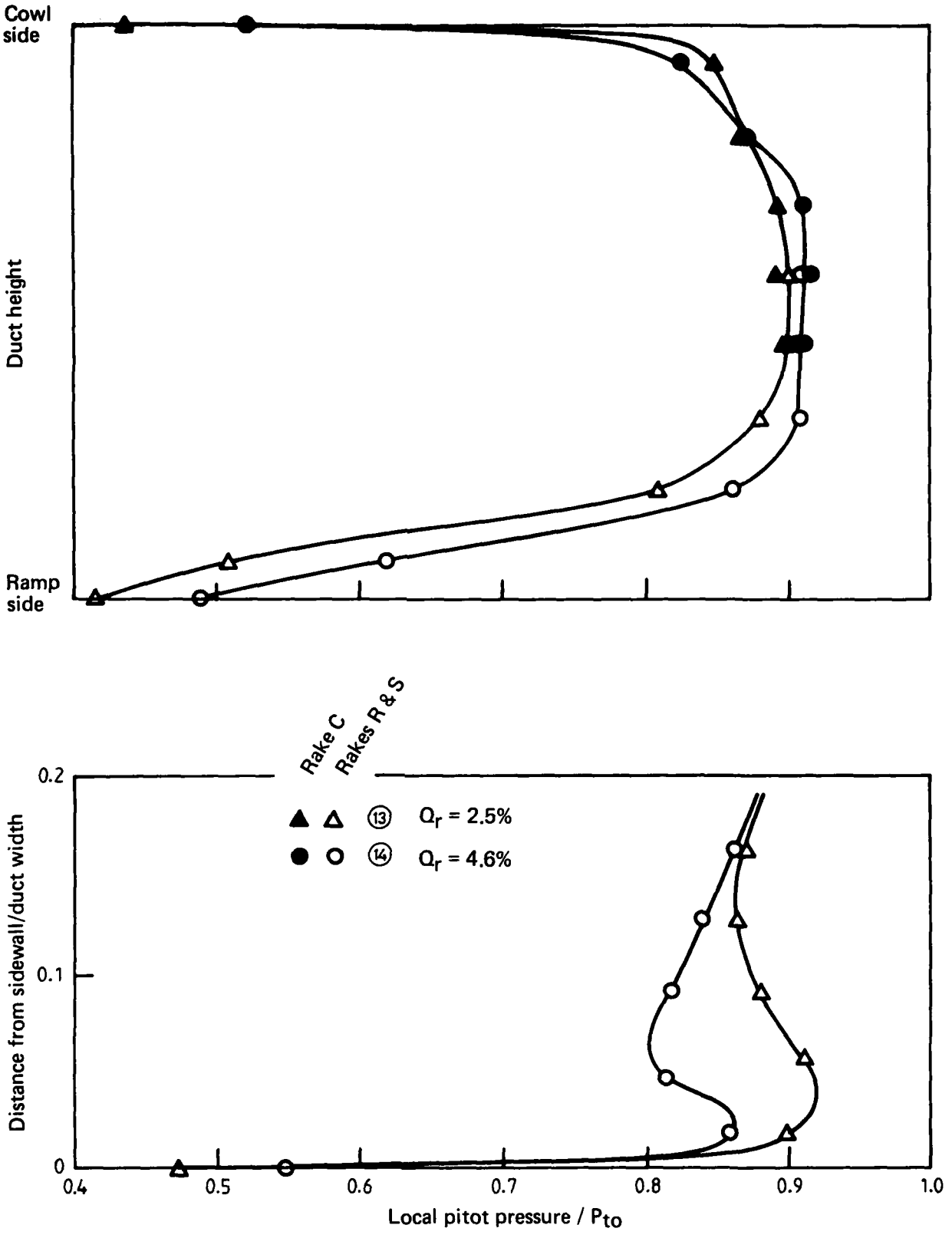

FIG. 25 EFFECT OF THROTTLING RAMP BLEED ON THROAT FLOW PROFILES – RAMP BLEED SLOT B, δ_2 = 8.2°, $t/_{Hi}$ = –0.002

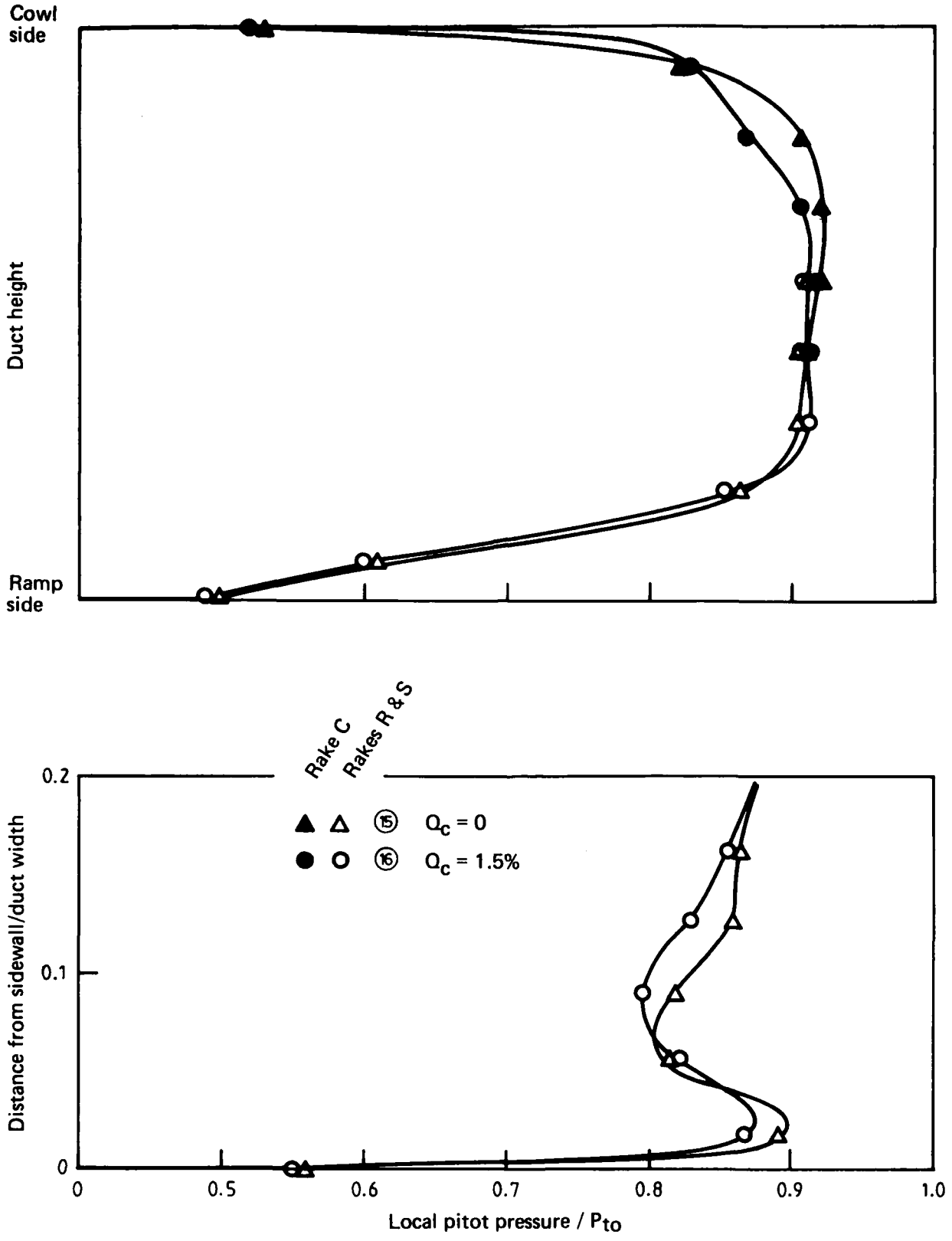

FIG. 26 EFFECT OF COWL BLEED FLOW ON THROAT FLOW PROFILES – RAMP BLEED SLOT B, $\delta_2 = 8.2°$, $t/_{Hi} = -0.002$

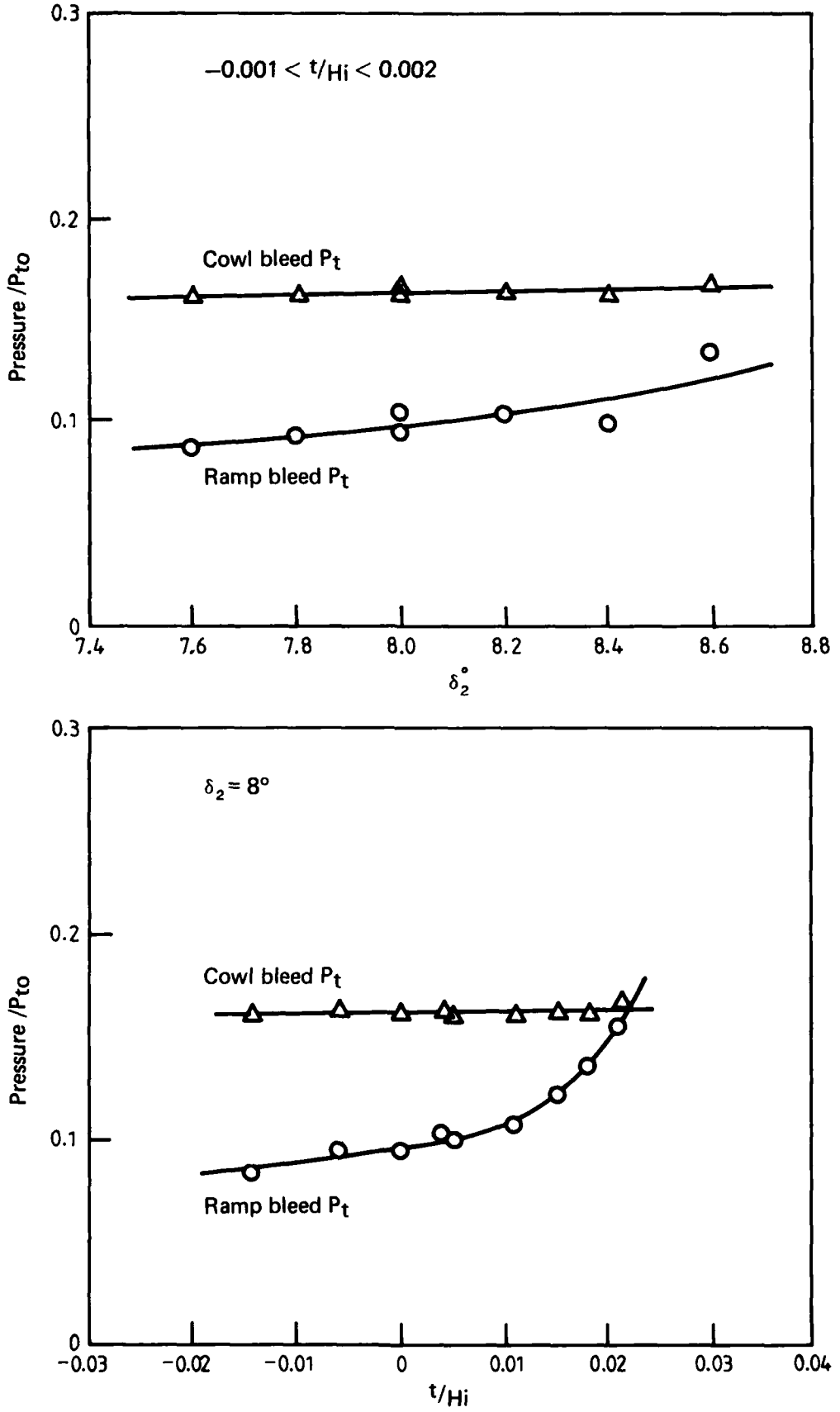

FIG. 27 BLEED PRESSURE RECOVERY – RAMP BLEED SLOT B

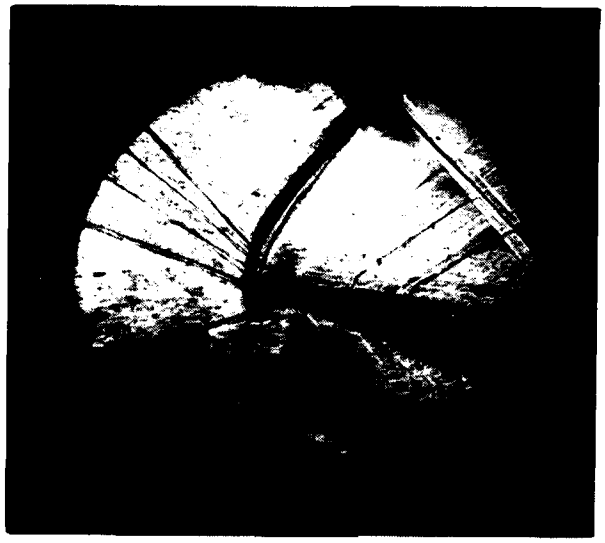

FIG. 28 THROAT FLOW IN CONFIGURATION C – δ_2 = 8°, $t/_{Hi}$ = 0.02, SUPERCRITICAL

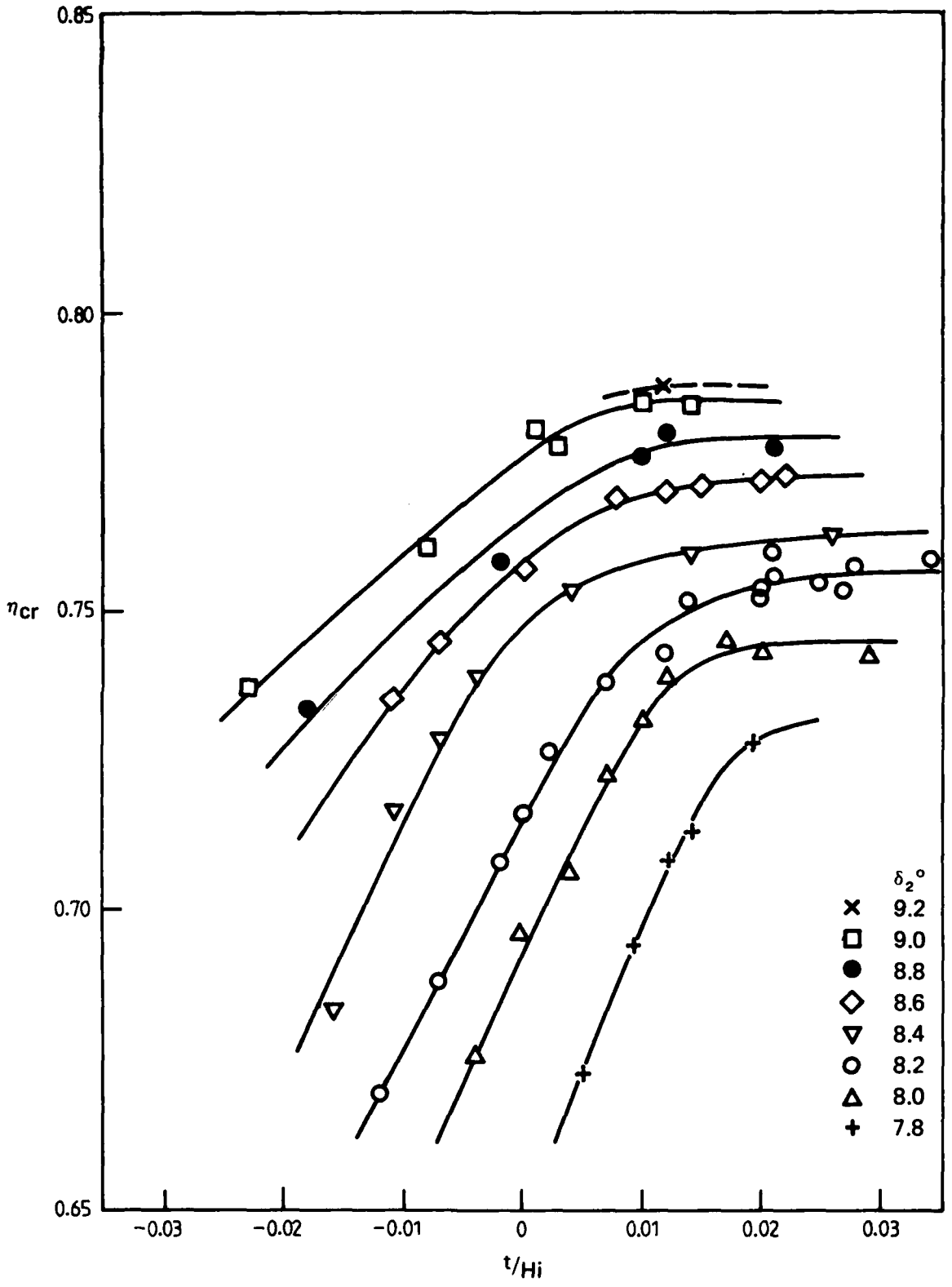

FIG. 29 EFFECT OF GEOMETRY ON PRESSURE RECOVERY – RAMP BLEED SLOT C

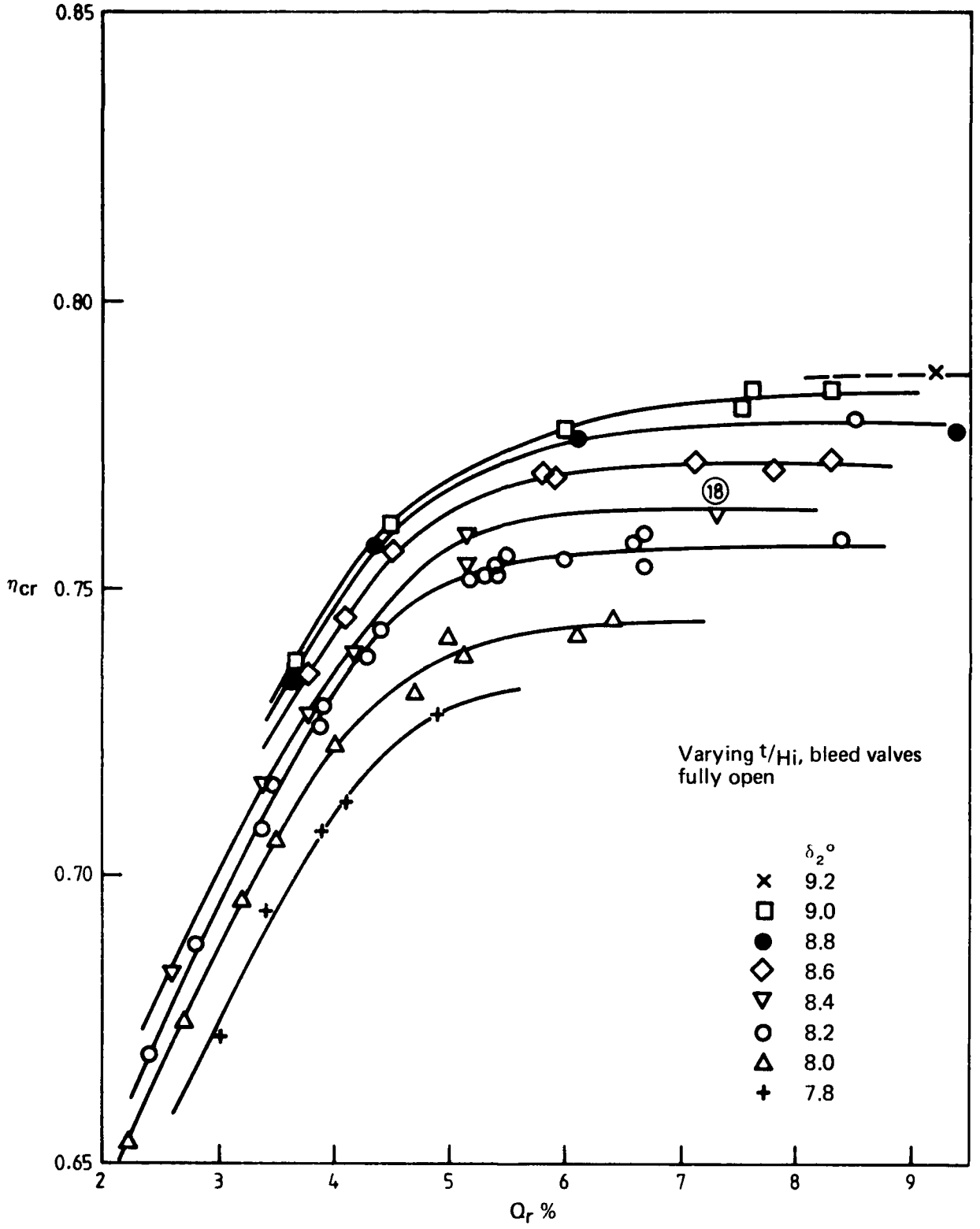

FIG. 30 EFFECT OF RAMP BLEED FLOW ON PRESSURE RECOVERY – RAMP BLEED SLOT C

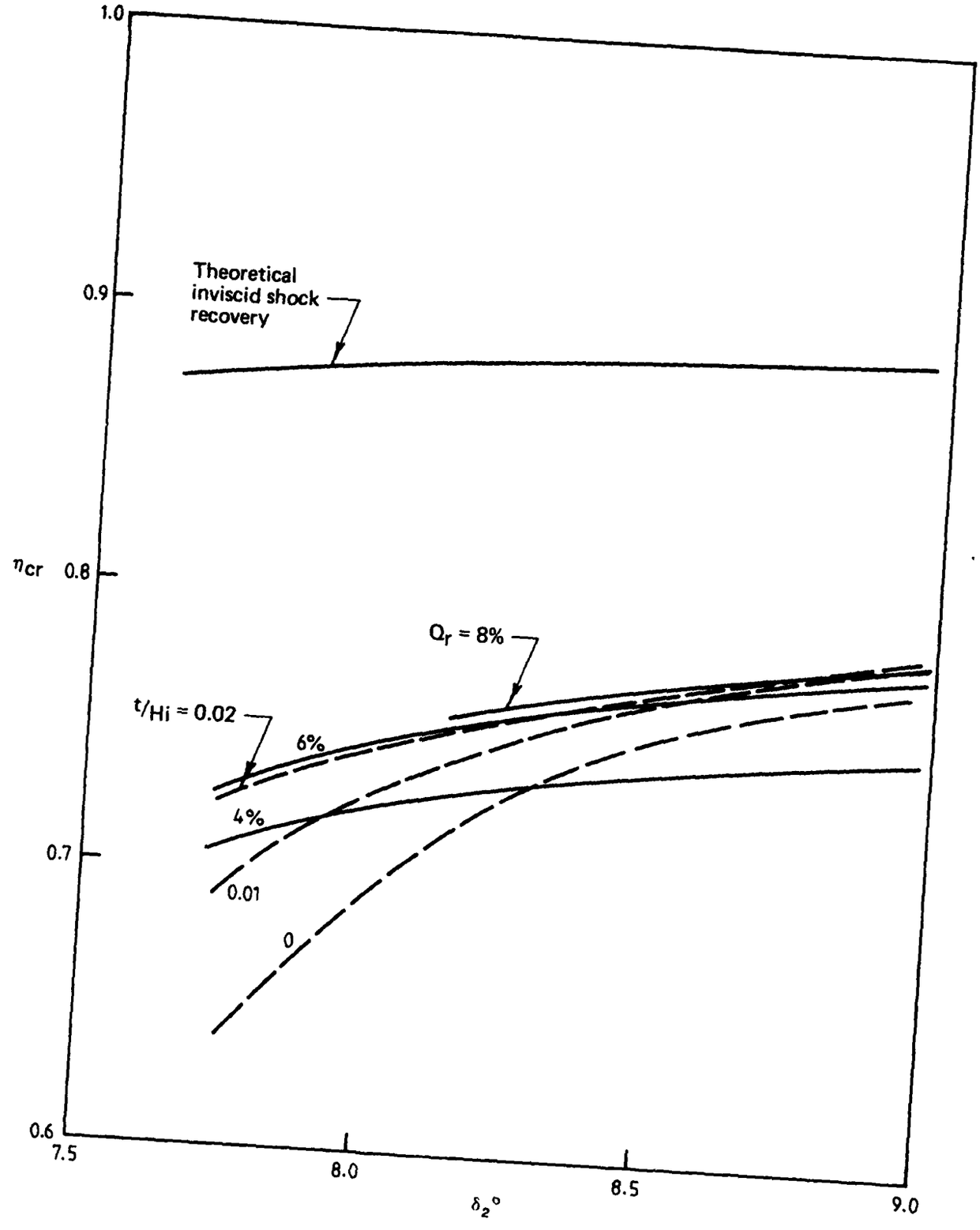

FIG. 31 MEASURED PRESSURE RECOVERY COMPARED WITH THEORETICAL SHOCK RECOVERY – RAMP BLEED SLOT C

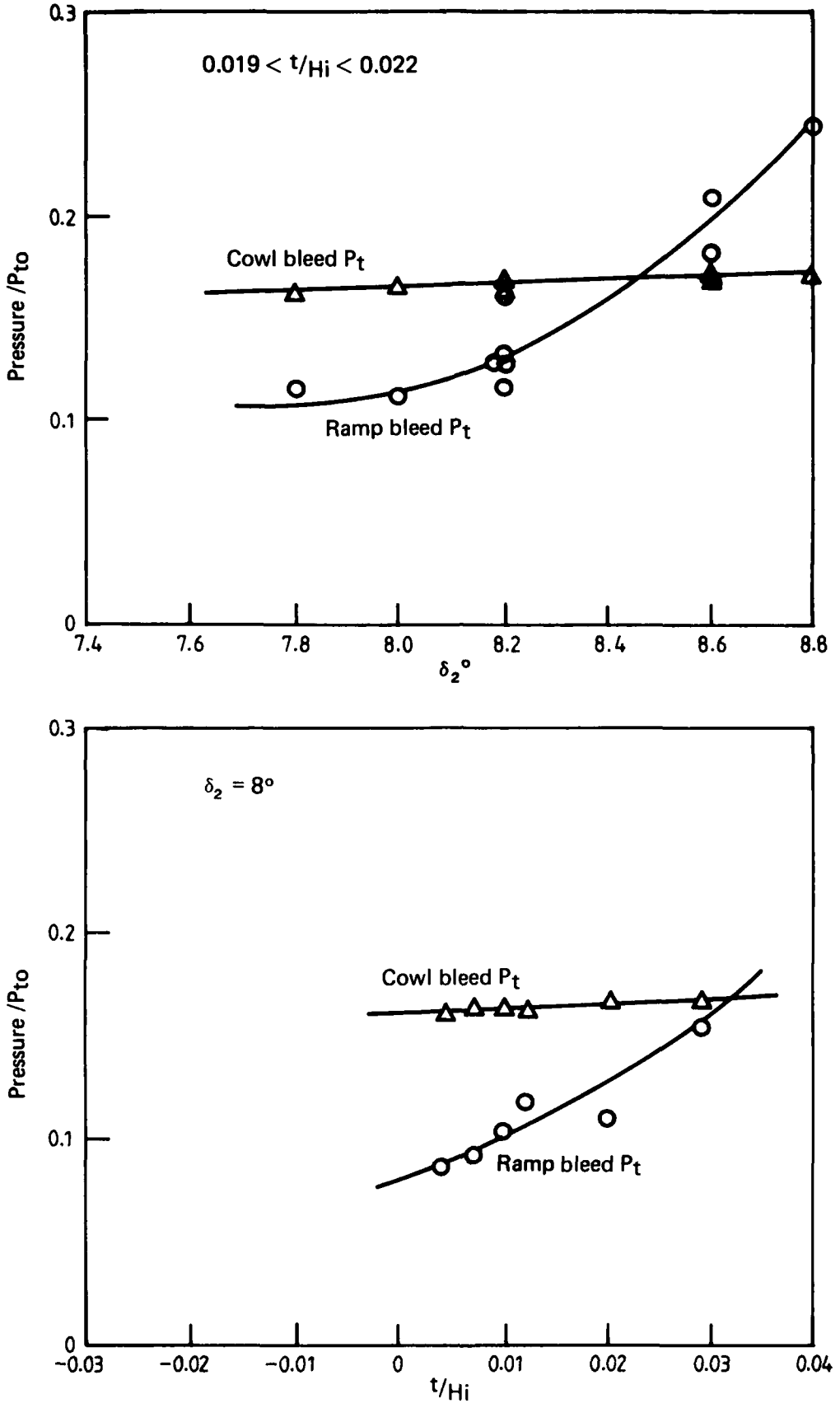

FIG. 32 BLEED PRESSURE RECOVERY – RAMP BLEED SLOT C

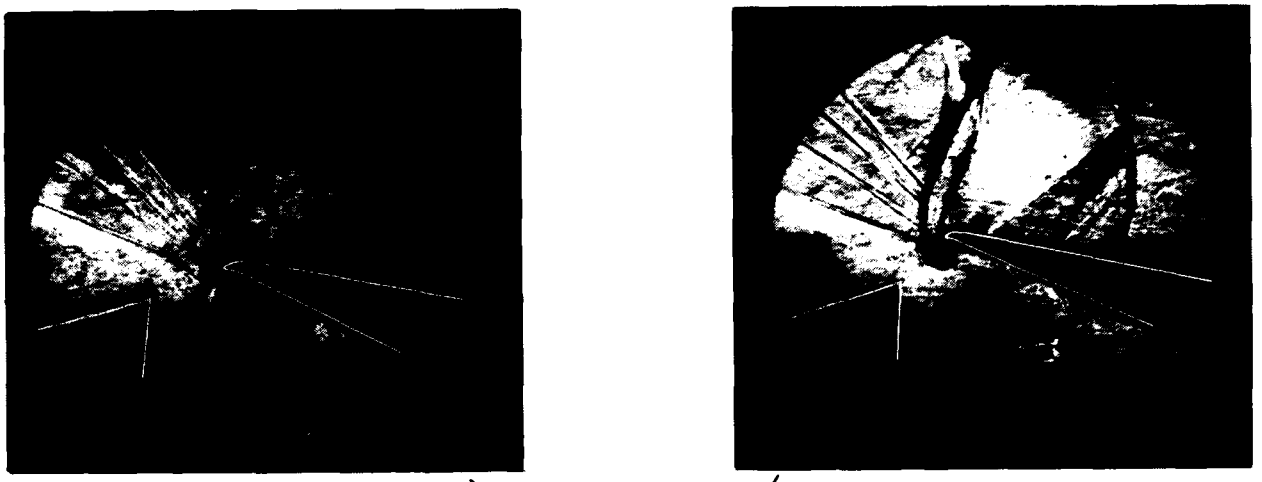

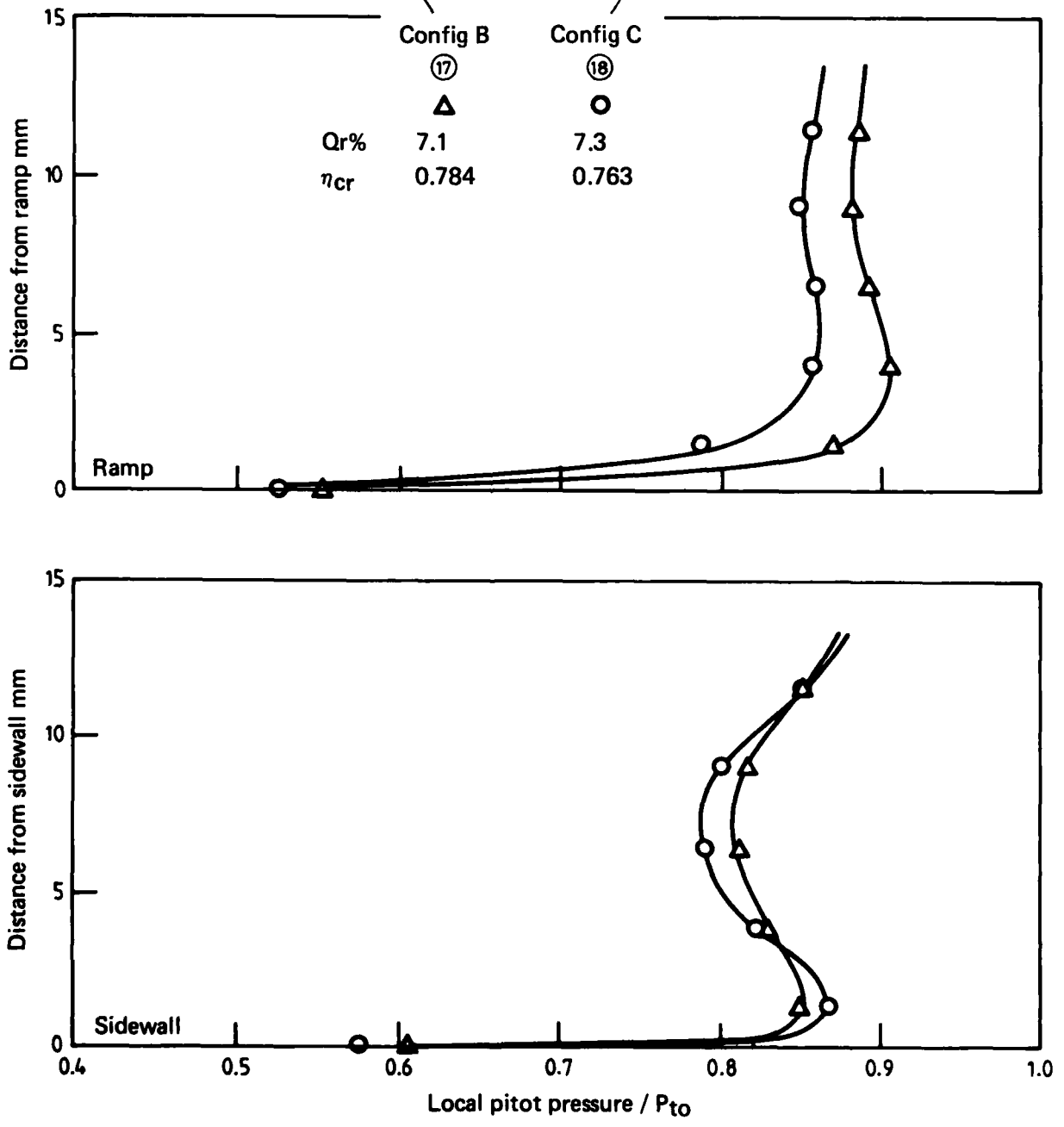

FIG. 33 COMPARISON OF THROAT FLOW – RAMP BLEED SLOTS B AND C, $\delta_2 = 8.4°$

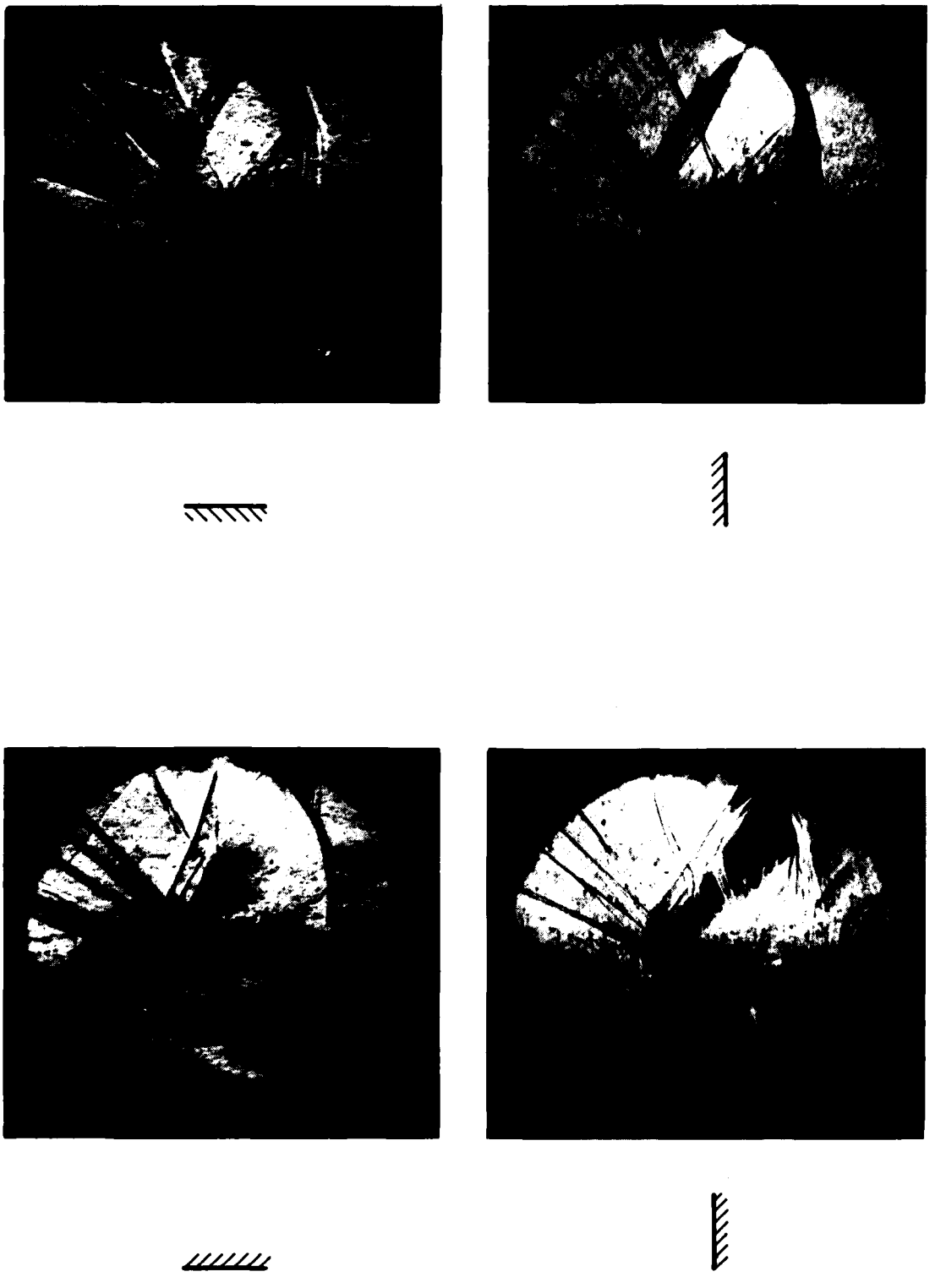

FIG. 34 SCHLIEREN PHOTOGRAPHS OF CRITICAL THROAT FLOW WITH VARIOUS CUT-OFF ORIENTATION – RAMP BLEED SLOT C, $\delta_2 = 8.2°$, $t/H_i = 0.02$

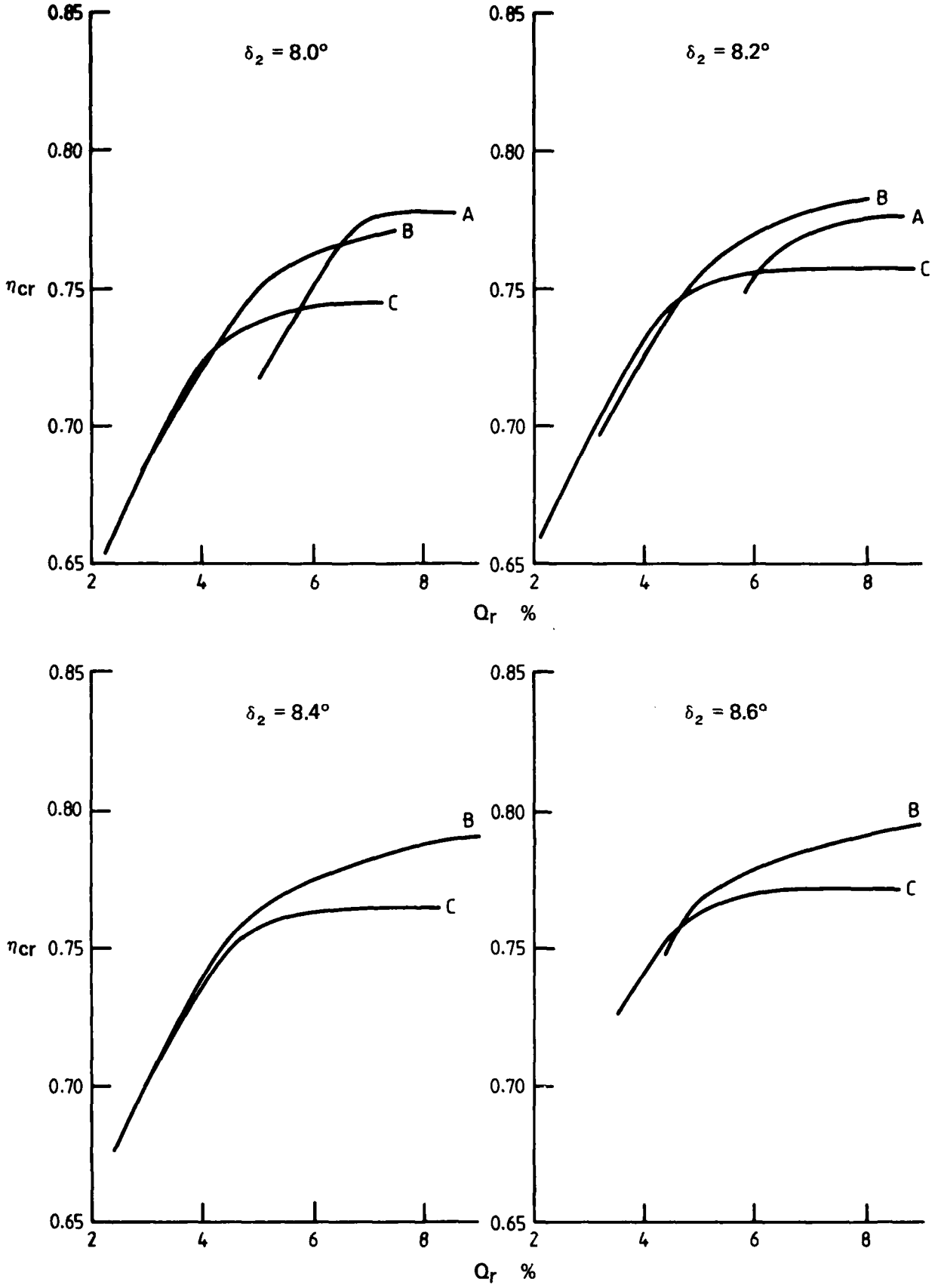

FIG. 35 COMPARATIVE PERFORMANCE OF CONFIGURATIONS A, B AND C – VARIABLE $t/_{Hi}$, BLEED VALVES FULLY OPEN

DISTRIBUTION

AUSTRALIA

DEPARTMENT OF DEFENCE

Defence Central

Chief Defence Scientist)
Deputy Chief Defence Scientist)
Superintendent, Science and Program Administration) (1 copy)
Controller, External Relations, Projects and Analytical Studies)
Defence Science Adviser (UK) (Doc Data sheet only)
Counsellor, Defence Science (USA) (Doc Data sheet only)
Defence Science Representative (Bangkok)
Defence Central Library
Document Exchange Centre, DISB (18 copies)
Joint Intelligence Organisation
Librarian H Block, Victoria Barracks, Melbourne

Aeronautical Research Laboratories

Director
Library
Superintendent - Aero Propulsion
Divisional File - Aero Propulsion
Author: S.A. Fisher

Materials Research Laboratories

Director/Library

Defence Research Centre

Library

RAN Research Laboratory

Library

Navy Office

Navy Scientific Adviser
Directorate of Naval Aircraft Engineering

Army Office

Scientific Adviser - Army
Engineering Development Establishment, Library

DISTRIBUTION (CONT'D)

Air Force Office

Air Force Scientific Adviser
Technical Division Library
Director General Aircraft Engineering - Air Force
RAAF Academy, Point Cook

Government Aircraft Factories

Library

DEPARTMENT OF AVIATION

Library

STATUTORY AND STATE AUTHORITIES AND INDUSTRY

Commonwealth Aircraft Corporation, Library
Hawker de Havilland Aust. Pty Ltd, Bankstown, Library

UNIVERSITIES AND COLLEGES

Adelaide	Barr Smith Library
Flinders	Library
La Trobe	Library
Melbourne	Engineering Library
Monash	Hargrave Library
Newcastle	Library
Sydney	Engineering Library
NSW	Physical Sciences Library
Queensland	Library
Tasmania	Engineering Library
Western Australia	Library
RMIT	Library

CANADA

NRC
Aeronautical & Mechanical Engineering Library

DISTRIBUTION (CONT'D)

UNIVERSITIES AND COLLEGES

Toronto — Institute for Aerospace Studies

CZECHOSLOVAKIA

Aeronautical Research and Test Institute (Prague), Head

FRANCE

ONERA, Library

INDIA

Defence Ministry, Aero Development Establishment, Library
Gas Turbine Research Establishment, Director
National Aeronautical Laboratory, Information Centre

JAPAN

Institute of Space and Astronautical Science, Library

NETHERLANDS

National Aerospace Laboratory (NLR), Library

NEW ZEALAND

Defence Scientific Establishment, Library

SWEDEN

Aeronautical Research Institute, Library

UNITED KINGDOM

CAARC, Secretary
Royal Aircraft Establishment
    Bedford, Library
    Pyestock North, Director
British Library, Lending Division
Aircraft Research Association, Library
Rolls-Royce Ltd, Aero Division Bristol, Library
British Aerospace
    Kingston-upon-Thames, Library
    Hatfield-Chester Division, Library

DISTRIBUTION (CONT'D)

UNIVERSITIES AND COLLEGES

Bristol	Engineering Library
Cambridge	Library, Engineering Department Whittle Library
Nottingham	Science Library
Southampton	Library
Liverpool	Fluid Mechanics Division, Dr J.C. Gibbings
Strathclyde	Library
Cranfield Inst. of Technology	Library
Imperial College	Aeronautics Library

UNITED STATES OF AMERICA

NASA Scientific and Technical Information Facility
United Technologies Corporation, Library
Lockheed-California Company
McDonnell Aircraft Company, Library

UNIVERSITIES AND COLLEGES

Massachusetts Inst. of Tech	MIT Libraries

SPARES (10 copies)
TOTAL (98 copies)

ADA 167005

Department of Defence

DOCUMENT CONTROL DATA

1. a. AR No	1. b. Establishment No	2. Document Date	3. Task No
AR-004-041	ARL-AERO-PROP-R-167	AUGUST 1985	DST 82/050

4. Title
INTERNAL PERFORMANCE OF A VARIABLE RAMP MIXED COMPRESSION INTAKE AT MACH 3.05

5. Security
a. document: UNCLASSIFIED
b. title: U c. abstract: U

6. No Pages

7. No Refs
11

8. Author(s)
S.A. FISHER

9. Downgrading Instructions

10. Corporate Author and Address
Aeronautical Research Laboratories
P.O. Box 4331,
Melbourne Vic 3001

11. Authority *(as appropriate)*
a.Sponsor b.Security c.Downgrading d.Approval

12. Secondary Distribution *(of this document)*
Approved for Public Release

Overseas enquirers outside stated limitations should be referred through ASDIS Defence Information Services Branch, Department of Defence, Campbell Park, CANBERRA ACT 2601

13. a. This document may be ANNOUNCED in catalogues and awareness services available to
No Limitations

13. b. Citation for other purposes *(ie casual announcement)* may be *(select)* unrestricted *(or)* as for 13 a

14. Descriptors
Air Intakes,
Boundary Layer Control,
Performance
Supersonic Inlets.

15. COSATI Group
01010
21010

16. Abstract

Results are presented of an experimental investigation into the performance of a two-dimensional mixed compression intake which featured focussed cowl compression matched to a discrete slot boundary layer bleed system. The tests were conducted at the intake design Mach number of 3.05. The design worked well in a two-dimensional sense, but the losses were exacerbated by three-dimensional viscous effects involving the sidewall boundary layers.

This page is to be used to record information which is required by the Establishment for its own use but which will not be added to the DISTIS data base unless specifically requested.

16. Abstract *(Contd)*

17. Imprint

Aeronautical Research Laboratories, Melbourne.

18. Document Series and Number	19. Cost Code	20. Type of Report and Period Covered
Aero Propulsion Report 167	42 7420	

21. Computer Programs Used

22. Establishment File Ref(s)

END

DTIC

5-86